

## Type list and selection guide

	Medical Imaging	Analytical & control	Physics	Type number	Size	Shape	Stage	Description	High energy resolution	Fast / Very fast	Low Noise	High count rate stability	High gain	Good linearity	Pages
NEW	✓	✓	✓	XP1302	13 mm	○	10-stage		→	↓	✓	✓	35		
NEW		✓		XP1302PC	13 mm	○	10-stage	photon-counting	→	↓	✓	✓	35		
NEW	✓			XP1303	13 mm	○	10-stage	red-sensitive	→		✓	✓	35		
	✓	✓		XP1308	13 mm	○	10-stage	UV-sensitive, quartz window	→		✓	✓	35		
NEW	✓	✓		XP1322	13 mm	○	10-stage	low-profile	→	↓	✓	✓	35		
NEW	✓			XP1322PC	13 mm	○	10-stage	low-profile, photon counting	→	↓	✓	✓	35		
NEW	✓	✓		XP1362	13 mm	○	6-stage		→		✓	✓	35		
NEW	✓	✓		XP1382	13 mm	○	8-stage		→		✓	✓	35		
	✓			XP1422	25 mm	□	11-stage	2-channel	✓				67		
	✓	✓	✓	XP1452	38 mm	□	11-stage	4-channel, individual channel gain adjustment	✓				67		
		✓		XP1802	230 mm	△	11-stage		⇒		✓	✓	69		
		✓		XP1803	130 mm	△	11-stage		⇒		✓	✓	69		
		✓		XP1804	270 mm	△	11-stage		⇒		✓	✓	70		
		✓		XP1805	230 mm	△	8-stage		⇒				70		
		✓		XP1806	203 mm	△	11-stage		⇒		✓	✓	71		
		✓		XP1807	300 mm	△	11-stage		⇒		✓	✓	71		
	✓	✓		XP1911	19 mm	○	10-stage		→			✓	36		
		✓		XP1911UV	19 mm	○	10-stage	UV-sensitive	→			✓	36		
	✓	✓		XP1912	19 mm	○	10-stage		✓	→	✓	✓	36		
		✓		XP1918	19 mm	○	10-stage	UV-sensitive, quartz window					36		
		✓		XP1921	19 mm	○	6-stage	green-sensitive	→				36		
		✓		XP1981	19 mm	○	8-stage	green-sensitive	→				36		
	✓	✓		XP2012	39 mm	○	10-stage					✓	43		
	✓			XP2013	39 mm	○	10-stage	red-sensitive				✓	43		
	✓			XP2015	39 mm	○	10-stage	infrared-sensitive				✓	43		
	✓			XP2016	39 mm	○	10-stage	high-temperature				✓	43		
	✓			XP2017	39 mm	○	10-stage	extended-red-sensitive				✓	43		
	✓			XP2018	39 mm	○	10-stage	UV-sensitive, quartz window				✓	43		
		✓		XP2020	51 mm	○	12-stage		→		✓	✓	47		
		✓		XP2020Q	51 mm	○	12-stage	UV-sensitive, quartz window	→		✓	✓	47		
		✓		XP2020UR	51 mm	○	12-stage	ultra fast	→		✓	✓	47		
		✓		XP2020URQ	51 mm	○	12-stage	UV-sensitive, quartz window, ultra fast	→		✓	✓	47		
NEW		✓		XP2040	39 mm	○	10-stage		✓			✓	44		
	✓			XP2042	39 mm	○	10-stage		✓			✓	44		
	✓			XP2060	39 mm	○	10-stage		✓			✓	44		
	✓			XP2062	39 mm	○	10-stage	15 pins foot base	✓	↓	✓	✓	44		
NEW	✓			XP20620	39 mm	○	10-stage			↓	✓	✓	44		
	✓			XP2072	39 mm	○	10-stage				✓		45		
	✓	✓		XP2090	39 mm	○	10-stage		→				45		
	✓			XP20A2	39 mm	○	10-stage	low-profile	✓	↓	✓	✓	45		
	✓	✓		XP20C2	39 mm	○	8-stage	low-profile	✓				45		
	✓	✓		XP20D0	51 mm	○	8-stage	double anode	✓	→			47		
NEW	✓	✓	✓	XP20H0	51 mm	○	10-stage	double anode	✓	→	✓		47		
	✓			XP2202	51 mm	○	10-stage						48		
	✓			XP2203	51 mm	○	10-stage	red-sensitive					48		
	✓			XP2220	51 mm	○	12-stage	high detection efficiency	⇒	↓		✓	48		
		✓		XP2242	51 mm	○	6-stage		⇒				48		
		✓		XP2254	51 mm	○	12-stage	UV to red-sensitive, quartz window	→			✓	49		
NEW		✓		XP2260	51 mm	○	12-stage		⇒			✓	49		
		✓		XP2262	51 mm	○	12-stage		⇒			✓	49		
		✓		XP2272	51 mm	○	12-stage	semi-fast	✓	⇒		✓	49		
		✓		XP2282	51 mm	○	8-stage		⇒			✓	49		
		✓		XP22K0	51 mm	○	12-stage	high detection efficiency	↓		✓		50		
		✓		XP2802	19 mm	○	10-stage		✓	↓	✓	✓	37		
NEW	✓			XP2802PC	19 mm	○	10-stage	photon counting	✓	↓	✓	✓	37		
	✓	✓		XP2812	19 mm	○	10-stage		⇒	↓		✓	37		
	✓			XP2822	19 mm	○	10-stage	low-profile	↓		✓	✓	37		
	✓			XP2822PC	19 mm	○	10-stage	photon counting	↓		✓	✓	37		
	✓	✓		XP2832	19 mm	○	10-stage	low-profile	⇒	↓	✓		37		
NEW	✓	✓		XP2882	19 mm	○	8-stage		⇒				37		

□: square - ○: round - △: hemispherical - ▽: hexagonal - □: dormer - ⇒: fast - →: very fast - ↓: low noise - ↘: very low noise

## Type list and selection guide

	Medical imaging	Analytical & control	Physics	Type number	Size	Shape	Stage	Description	High energy resolution	Fast / Very fast	Low Noise	High count rate stability	High gain	Good linearity	Pages
NEW	✓			XP2900	29 mm	○	10-stage		➡			✓			41
		✓		XP2901	29 mm	○	10-stage	green-sensitive	➡			✓			41
	✓			XP2920	29 mm	○	11-stage			↳		✓			41
	✓			XP2920PC	29 mm	○	11-stage	photon counting		◀		✓			41
	✓			XP2930	29 mm	○	11-stage	low-profile		↳		✓			41
	✓			XP2940	29 mm	○	11-stage			↳		✓			41
NEW	✓			XP2950	29 mm	○	11-stage	low-profile		↳		✓			41
	✓			XP2950PC	29 mm	○	11-stage	photon counting		◀		✓			41
NEW	✓			XP29507	29 mm	○	7-stage	low-profile							41
NEW	✓			XP29508	29 mm	○	8-stage	low-profile							41
NEW	✓			XP2960	29 mm	○	8-stage		➡						42
		✓		XP2970	29 mm	○	10-stage	UV-sensitive	➡						42
	✓			XP2972	29 mm	○	10-stage		➡						42
		✓		XP2978	29 mm	○	10-stage	UV-sensitive, quartz window	➡						42
	✓			XP3060	39 mm	○	7-stage		→						46
		✓		XP3062	40 mm	○	8-stage	cosmic-ray air shower telescope PMT				✓			74
NEW	✓			XP3100	25 mm	○	10-stage	UV-sensitive	➡						38
NEW	✓			XP3100D	51 mm	○	12-stage	ruggedized, high temperature	➡		✓				50
NEW	✓			XP3100C	51 mm	○	12-stage	ruggedized, high temperature	➡		✓				50
NEW	✓			XP31034	51 mm	○	11-stage	reflection mode, high sensitivity, GaAs	➡	↳		✓			50
NEW	✓			XP31034/02	51 mm	○	11-stage	reflection mode, high sensitivity, GaAs	➡	↳		✓			50
NEW	✓			XP31034/06	51 mm	○	11-stage	reflection mode, high sensitivity, GaAs	➡	↳		✓			50
NEW	✓			XP31034A	51 mm	○	11-stage	reflection mode, high sensitivity, GaAs	➡	↳		✓			50
NEW	✓			XP31034A/02	51 mm	○	11-stage	reflection mode, high sensitivity, GaAs	➡	↳		✓			50
NEW	✓			XP31034A/05	51 mm	○	11-stage	reflection mode, high sensitivity, GaAs	➡	↳		✓			50
NEW		✓		XP3108	25 mm	○	10-stage	UV-sensitive, quartz window	➡						38
	✓			XP3110	25 mm	○	10-stage	low-profile	➡	↳					38
	✓			XP3110PC	25 mm	○	10-stage	photon counting	➡	↳					38
				XP3132	25 mm	○	10-stage								38
		✓		XP3162	25 mm	○	6-stage	low-profile	➡						39
		✓		XP3182	25 mm	○	8-stage	low-profile	➡						39
NEW	✓	✓		XP31S2	25 mm	○	10-stage	low-profile	➡						39
	✓	✓		XP31SF	25 mm	○	10-stage	low-profile, flying-leads	➡	↳					39
	✓	✓		XP3212	51 mm	○	8-stage			✓					51
NEW		✓		XP3230	51 mm	○	10-stage			✓	↳		✓		51
	✓			XP3232	51 mm	○	10-stage			✓					51
	✓			XP3292	51 mm	□	8-stage			✓					65
NEW	✓			XP32K0	51 mm	○	10-stage			✓	◀		✓		51
	✓			XP3312	76 mm	○	8-stage			✓					55
	✓			XP3330	76 mm	○	10-stage			✓	↳		✓		55
	✓			XP3332	76 mm	○	10-stage			✓					55
	✓			XP3372	76 mm	○	8-stage			✓					55
	✓			XP3392	76 mm	□	8-stage			✓					55
NEW	✓			XP33K0	76 mm	○	10-stage			✓	◀		✓		55
		✓		XP3462	76 mm	○	8-stage		➡				✓		56
		✓		XP3468	76 mm	○	8-stage	UV-sensitive, quartz window	➡				✓		56
	✓			XP3540	130 mm	○	10-stage			✓	↳		✓		61
	✓			XP35K0	130 mm	○	10-stage			✓	◀		✓		61
	✓			XP3612	60 mm	○	8-stage			✓					54
NEW	✓			XP3672	60 mm	○	8-stage			✓					64
	✓			XP3712	90 mm	○	8-stage			✓					59
	✓			XP3730	90 mm	○	10-stage			✓	↳		✓		59
	✓			XP3732	90 mm	○	10-stage			✓			✓		59
	✓			XP3762	90 mm	○	6-stage								59
	✓			XP37K0	90 mm	○	10-stage			✓	◀		✓		59
NEW	✓	✓		XP3990	29 mm	□	9-stage			✓					65
	✓			XP4312	76 mm	○	12-stage		➡			✓			56
	✓			XP4318	76 mm	○	12-stage	UV-sensitive, quartz window	➡			✓			56
	✓			XP4362	76 mm	○	6-stage		➡						56
	✓			XP4372	76 mm	○	8-stage		➡			✓			56
	✓			XP4392	76 mm	○	10-stage		➡		✓	✓			56

□: square - ○: round - △: hemispherical - ○: hexagonal - □: dormer - ➡: fast - →: very fast - ↳: low noise - ↲: very low noise

## Type list and selection guide

	Medical imaging	Analytical & control	Physics	Type number	Size	Shape	Stage	Description	High energy resolution	Fast / Very fast	Low Noise	High count rate stability	High gain	Good linearity	Pages
NEW	✓			XP4500	130 mm	○	10-stage	UV-sensitive	➡			✓	✓		62
	✓			XP4508	130 mm	○	10-stage	UV-sensitive, quartz window	➡			✓	✓		62
		✓		XP4512	130 mm	○	10-stage		➡			✓	✓		62
	✓			XP4526A	39 mm	□	10-stage	red-sensitive, dormer window							64
		✓		XP4572	130 mm	○	10-stage	semi-fast	✓	➡		✓	✓		62
		✓		XP4592	130 mm	○	8-stage		➡				✓		63
		✓		XP5200	51 mm	○	8-stage	low-profile	✓		✓				52
		✓		XP5202	51 mm	○	8-stage	low-profile	✓		✓				52
	✓			XP5292	51 mm	□	9-stage	low-profile	✓						66
	✓	✓		XP52Y2	51 mm	○	8-stage	low-profile	✓	➡					52
NEW				XP5300	76 mm	○	8-stage	low-profile	✓						57
NEW	✓			XP5302	76 mm	○	8-stage	low-profile	✓		✓				57
NEW	✓			XP5382	76 mm	□	8-stage	low-profile	✓		✓				66
NEW	✓			XP53A2	76 mm	○	6-stage	low-profile	✓	➡					57
NEW	✓	✓		XP53X2	76 mm	○	9-stage	low-profile	✓	➡		✓			57
NEW	✓	✓		XP53Y2	76 mm	○	8-stage	low-profile	✓	➡					57
NEW	✓			XP5612	60 mm	○	9-stage		✓						54
NEW				XP5700	90 mm	○	8-stage	low-profile	✓						60
NEW	✓			XP6042	39 mm	○	10-stage	low-profile							46
NEW				XP6242	51 mm	○	10-stage	very low-profile							52
NEW				XP6342	76 mm	○	10-stage	very low-profile							57
NEW				XP6500	13 mm	○	9-stage	very low-profile							35
NEW				XP650F	13 mm	○	9-stage	very low-profile, flying-leads							35
NEW	✓			XP83006	130 mm	○	10-stage	good PHR	✓						63
NEW	✓	✓		XP83013	90 mm	○	10-stage		✓						60
NEW	✓			XP83019	51 mm	○	10-stage		✓						53
NEW	✓			XP83021	76 mm	○	10-stage		✓						58
NEW	✓	✓		XP83049	76 mm	○	8-stage	green-sensitive	✓		✓				58
NEW	✓			XP83051C	25 mm	○	10-stage	ruggedized, high temperature							40
NEW	✓			XP83051E	25 mm	○	10-stage	ruggedized, high temperature							40
NEW	✓	✓		XP83054	51 mm	○	8-stage	green-sensitive	✓		✓				53
NEW	✓	✓		XP83079	76 mm	□	8-stage	green-sensitive	✓		✓				66
NEW	✓			XP83092C	25 mm	○	10-stage	ruggedized, high temperature							40
NEW	✓			XP83092E	25 mm	○	10-stage	ruggedized, high temperature							40
NEW	✓	✓		XP83112	25 mm	○	10-stage		✓	➡		✓			40
NEW	✓	✓	✓	XP83120	29 mm	○	10-stage		✓	➡		✓			42
NEW	✓	✓		XP83121	29 mm	○	10-stage	red-sensitive	➡						42
NEW	✓	✓		XP85002	51 mm	□	2-MCP	MCP multiplier, 4 anode	➡						68
NEW	✓	✓		XP85012	51 mm	□	2-MCP	MCP multiplier, 64 anode	➡						68
NEW	✓	✓		XP85022	51 mm	□	2-MCP	MCP multiplier, 1024 anode	➡						68
NEW	✓	✓	✓	XP8850	51 mm	○	12-stage	Quantacon	➡	🔊	✓	✓			53
NEW	✓			XP8852	51 mm	○	12-stage	red-sensitive, Quantacon	➡		✓	✓	✓		53

□: square - ○: round - ▲: hemispherical - ◻: hexagonal - □: dormer - ➡: fast - ➔: very fast - 🔊: low noise - 🔋: very low noise

Imperial sizes: in this catalogue, the following size equivalents are used.

½"	13 mm	1 1/8"	29 mm	2 1/4"	57 mm	3 1/2"	90 mm	9"	230 mm
¾"	19 mm	1 ½"	39 mm	2 ½"	60 mm	5"	130 mm	10 ½"	270 mm
1"	25 mm	2"	51 mm	3"	76 mm	8"	203 mm	12"	300 mm

## ■ Still setting the standard



For more than sixty years, photomultipliers have been used to detect low-energy photons in the UV to visible range, high-energy photons (X-rays and gamma rays) and ionizing particles using scintillators. PHOTONIS has been manufacturing them from their inception. Today, photomultiplier tubes (PMT) remain unequalled in light detection in all but a few niche areas.

The PMT's continuing superiority stems from three main features:

- large sensing area,
- ultra-fast response and excellent timing performance,
- high gain and low noise.

The last two give the photomultiplier an exceptionally high gain-bandwidth product.

For detecting light from UV to visible wavelengths, the PMT has successfully met the challenges of solid-state light detectors such as the silicon photodiode and the silicon avalanche photodiode. Detectors of this sort have only made minor inroads into some traditional PMT markets where the light levels are relatively high and a small sensing area can be tolerated.

For detecting high-energy photons or ionizing particles, the PMT remains widely preferred. It continues to compete effectively with solid-state radiation detectors and gaseous detectors (though the former can provide superior energy resolution to PMT scintillation counters in some areas of X-ray and low-energy gamma-ray spectrometry).

And in large-area detectors, the availability of scintillating fibres is again favouring the use of the PMT as an alternative to the slower multi-wire proportional counter. Not that development of the PMT itself has been standing still. For example, to meet today's increasingly stringent demands in nuclear imaging, PHOTONIS is constantly refining existing designs to raise performance while making ever smaller tubes.

And for the analytical and physics markets, PHOTONIS has developed completely new technologies such as the broadly-patented foil dynode that is the key to the low-crosstalk of the latest multi-channel PMT family. Then there are very large hemispherical PMTs with excellent time response for cosmic ray experiments, and ultra-fast tubes with a time jitter of less than half a nanosecond. And this is just a few of the unequalled products listed in this catalogue from the company setting the standard in photomultiplier tubes.

## ■ Construction & operating principle

A photomultiplier tube is a non-thermionic vacuum tube, usually made of glass, that converts very small light signals into a measurable electric current.

As Fig.1 shows, it comprises:

- a **window** to admit light,
- a **semitransparent photocathode** made of a thin layer of photoemissive material deposited on the inner surface of the window which emits electrons in response to absorbing photons,
- an **electron-optical input system** of one or more electrodes that accelerate and focus the emitted photoelectrons onto the first dynode of the tube,
- an **electron multiplier** consisting of several electrodes (dynodes) covered with a layer of secondary emissive material. For each incident electron, each dynode emits several secondary electrons. These are accelerated onto the next dynode by an inter-dynode potential (typically of about 100 V) producing ever more secondary electrons down the multiplier. Electron gains of  $10^3$  to  $10^8$  are common and depend on the number of dynodes and the inter-dynode potentials,
- an **anode grid** which collects the electron avalanche, providing an output signal.

The electrode potentials are usually derived from a single high-voltage supply and a resistive or transistorized voltage divider.

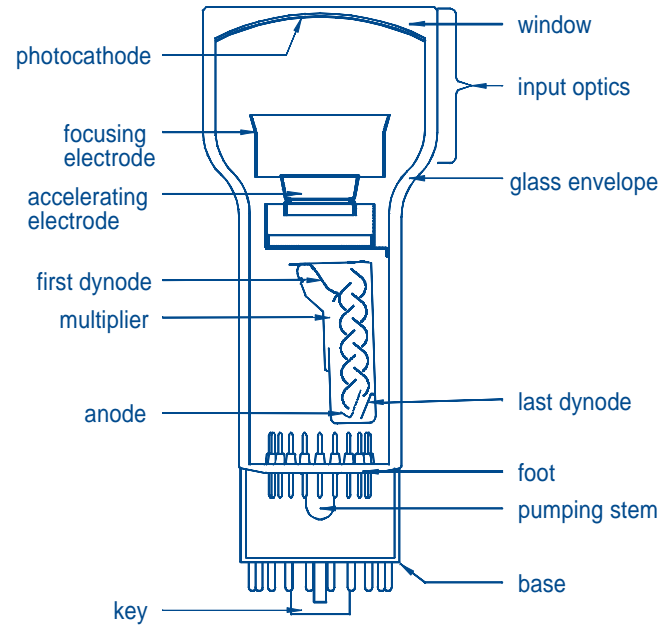


**Fig.1:** Main elements of a photomultiplier.  
(Based on the fast 3" basic tube, the XP4312B).

# The photocathode

The response of a PMT to light is specified by its photocathode sensitivity which can be specified by several ways: quantum efficiency, integral quantum efficiency, cathode radiant sensitivity, cathode luminous sensitivity and cathode blue sensitivity.

## Quantum efficiency (%)

Quantum efficiency (QE, or  $\rho$ ) is the most obvious way to describe cathode photoemission. It is defined as the ratio of the number of photoelectrons emitted by the cathode to the number of photons incident on the window, and is usually expressed as a percentage.

Quantum efficiency depends on the wavelength of the photons and is generally less than 35%. For each photocathode type, a range of wavelengths in which the QE has a usable value can be defined, the lower limit of QE (and hence the measuring accuracy) being set by the statistical nature of photoemission.

Quantum efficiency is a particularly useful parameter when the number of incident photons is small and when the photons arrive in pulses.

## Cathode radiant sensitivity (mA/W)

Because it is easier to measure the photocathode current produced in response to an incident light power than to count photons and electrons, photoemission is frequently described by the term cathode radiant sensitivity and is usually expressed in mA/W. This sensitivity is the photocathode current produced in response to an incident light power at a specific wavelength.

Cathode radiant sensitivity is related to quantum efficiency by:

$$QE (\%) = \frac{124}{\lambda \text{ (nm)}} \times \text{radiant sensitivity (mA/W)}$$

where  $\lambda$  is the wavelength of the incident light.

## Spectral response

The spectral sensitivity characteristic (Fig.2) is the curve showing how cathode radiant sensitivity varies with wavelength. The spectral response is determined at the longer wavelengths (photoemission threshold) by the photocathode type and thickness, and at the shorter wavelengths by the input window transmission.

## Window material

The most commonly used window materials are (Fig.3):

- **lime glasses** (soft glasses), e.g. Schott B270,
- **borosilicate glasses** (hard glasses), e.g. Corning Pyrex™,
- **UV-transparent borosilicate glasses**, e.g. Schott 8337,
- **fused silica**, e.g. Spectrosil™, which is very transparent to UV radiation down to about 160 nm.
- **sapphire (ultraviolet grade)**

Within each group of glass, there are many variants having different transmissions.

## Characteristics of photomultiplier windows

type of window glass	cut-off wavelength, -10% (nm)	refractive index
lime glass	300	1.54 (at 400 nm)
borosilicate	270	1.50 (at 400 nm)
UV glass	190	1.49 (at 400 nm)
fused silica	160	1.47 (at 400 nm)
		1.50 (at 250 nm)
sapphire	150	1.80 (at 400 nm)

The window material choice has other consequences which may be critical for some applications (see p 15).

Alpha, beta and gamma decays within the materials of a photomultiplier (glass, insulator, metal parts) can produce interactions with scintillators. These interactions can lead to events with time and energy signatures which can mislead with the rare events being studied (see p 14).

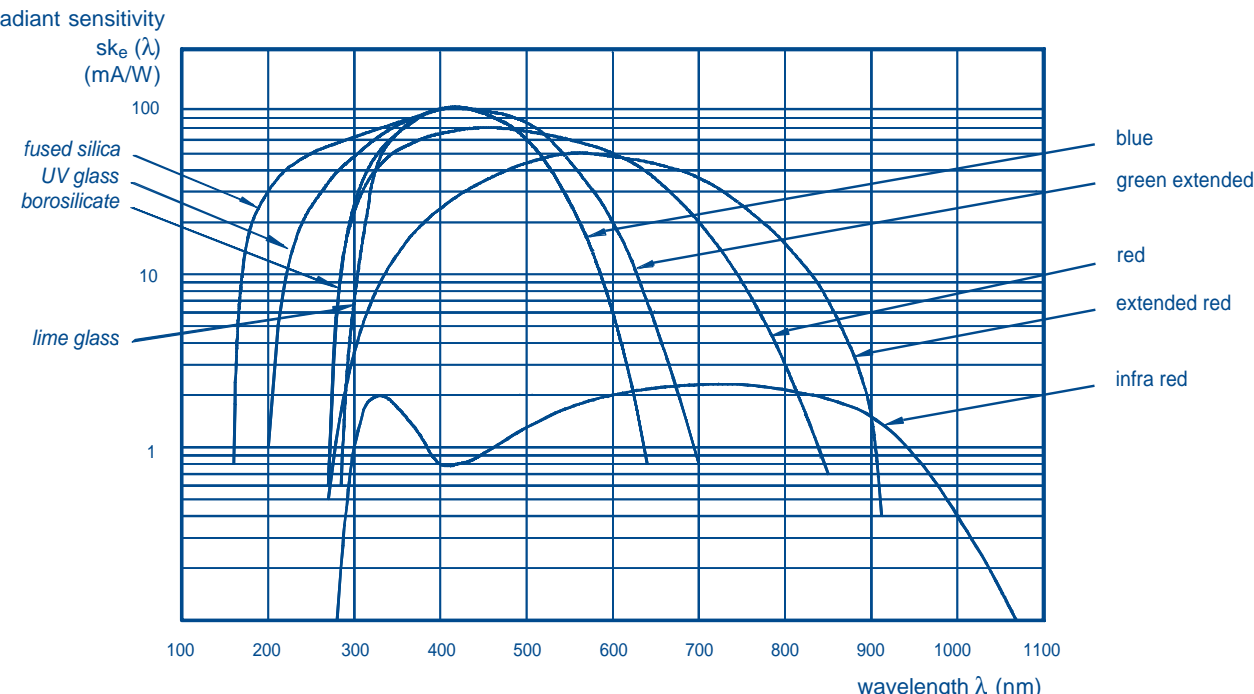
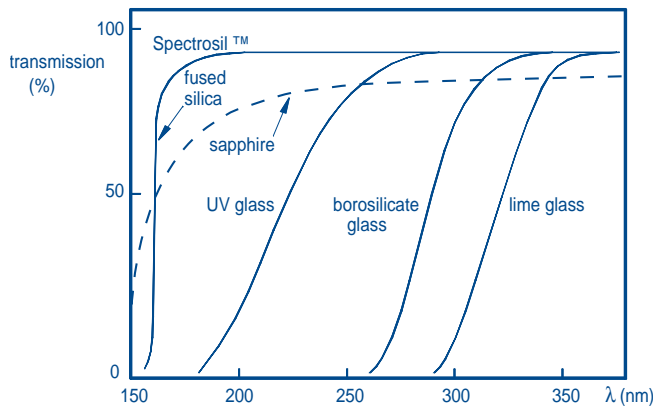


Fig.2 Typical spectral sensitivity characteristics of standard photocathodes with associated window materials.



**Fig.3** Transmission as a function of wavelength  $\lambda$  for various glasses used in photomultiplier input windows.

### Photocathode material

PMT photocathodes are usually made of alkali antimonides, the most common being:

- **bialkali** (SbKCs): used to match light sources in the blue region of the visible spectrum,
- **green-extended bialkali** (GEBA): more sensitive than standard bialkali in the green region,
- **high-temperature bialkali** (SbNa<sub>2</sub>K): less sensitive than the other bialkali cathodes; for prolonged use at temperatures above 60°C,
- **multialkali** (SbNa<sub>2</sub>KCs): more sensitive than the bialkali types in the range 600 to 850 nm, but with correspondingly higher noise,
- **extended-red multialkali** (ERMA): a thicker multialkali cathode whose spectral response extends to 900 nm,
- **GaAs**, near infrared sensitive
- **RbCsSb**.

The response of the multialkali cathodes can be tailored to extend as required in the green and red regions.

Other rarely used photocathode types are:

- the monoalkali cathode (SbCs<sub>3</sub>),
- the AgOCs cathode which is sensitive from the visible region to the infrared region, but has a very low QE,
- alkali tellurides on fused silica ('solar blind').

### Luminous and filtered sensitivities

Because it would be prohibitively expensive (and indeed irrelevant for most applications) to measure the spectral sensitivity characteristic of every PMT, individual PMTs are usually only tested for minimum sensitivity. Further more, for historical and practical reasons, neither quantum efficiency nor radiant sensitivity is measured.

All major PMT manufacturers have instead standardized tests according to well-known techniques used in the lighting industry where light flux is measured in lumens (reflecting the response of the ideal human eye) and not in watts, and where the spectral response is measured for a tungsten filament light source at a colour temperature of 2856K.

Because the spectral response of a PMT is much wider than that of the eye, the use of such photometric measurements has often been criticized. However, the definition of the lumen is directly related to a few practical physical parameters (dimensions of a tungsten filament, emissivity of tungsten, colour temperature) that are easy to control and calibrate, providing reliable and reproducible test results.

### Cathode luminous sensitivity ( $\mu\text{A/lm}$ )

Cathode luminous sensitivity relates the photocathode current to the response of the ideal eye. It is the current measured for an incident flux of 1 lumen from a tungsten filament source at a colour temperature of 2856K. It is usually expressed in  $\mu\text{A/lm}$ .

The luminous sensitivity can be considered as the integral product of the cathode spectral response and the radiant power spectrum of the light source. Therefore, high values of luminous sensitivity correspond very well to an extended green response. Thus, it is a useful characteristic to specify and is indicated on the test ticket of all PHOTONIS tubes having an extended response, i.e. those with GEBA, multialkali, or ERMA cathodes. For PMTs with a multialkali cathode, the radiant sensitivity at a specified wavelength is also indicated.

### Luminous filtered sensitivity ( $\mu\text{A/lmF}$ )

This is measured with the same standard light source as luminous sensitivity but with a colour filter placed between the source and PMT to simulate the emission spectrum of another source, mostly a scintillator.

The most widely used filter is the Corning CS 5-58, polished to half-stock thickness, which closely simulates the emission of NaI(Tl), see Fig.4. The photocathode current corresponding to 1 lumen incident on this filter is called cathode blue sensitivity or cathode CB sensitivity (CB for Corning Blue), and is expressed in  $\mu\text{A/lmF}$  (F for filtered). It is used by all PMT manufacturers to specify and test PMTs intended for use with NaI(Tl) scintillators. Individual measured values are indicated on the test ticket of every PHOTONIS PMT with a bialkali photocathode.

The 'blue' and radiant sensitivities at 400 nm are empirically related for a standard bialkali photocathode:

$$\text{radiant sensitivity at } 400 \text{ nm} \approx 8 \times \text{blue sensitivity} \quad (\text{mA/W}) \quad (\mu\text{A/lmF})$$

### Integral quantum efficiency (%)

For many physics applications using green-emitting scintillators or wavelength shifters with a well-defined emission band, the integral quantum efficiency (IQE) is a useful parameter to express cathode sensitivity. It is defined as the integral product of the photocathode spectral sensitivity characteristic and the light emission spectrum and is expressed as a percentage.

The IQE is well correlated with the photocathode luminous sensitivity given on the test ticket of all GEBA, multialkali and ERMA tubes. If the emission spectrum of the light is known, the IQE can be approximated from the photocathode response of a typical PMT and the emission spectrum of the standard light source used in measuring luminous sensitivity.

For wavelength shifters such as BBQ, Y7 and Y27, coupled to an XP2072 photomultiplier, the IQE is typically 10-15%, for the green-extended XP1921 typically 12-18%, and for recent tubes for gamma-cameras typically 15-20%.

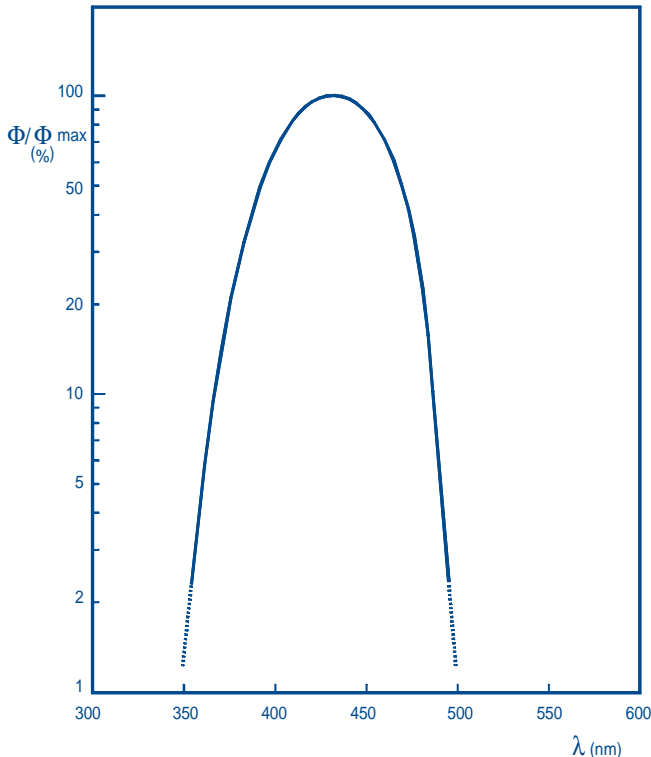


**Fig.4** Relative spectral characteristic of 2856 K tungsten light transmitted by a Corning CS 5-58 filter ground to half stock thickness.

### Measuring cathode sensitivity

All published cathode sensitivities are measured by operating the PMT as a diode with all electrodes in the input optics interconnected. This optimizes collection efficiency, so the measurement is a true indication of cathode quality (especially useful for manufacturers' process control). Cathode sensitivities do not however indicate the collection efficiency during normal operation as a photomultiplier, see Collection Efficiency.

### Spatial uniformity

Reproducible, high-quality deposition techniques ensure that the spatial uniformity of the cathode sensitivity of PHOTONIS end-window PMTs is excellent. Minute variations may however be perceptible if uniformity measurements are made using a light source outside the PMT's intended spectral operating range, e.g. using a green or red LED to measure a PMT optimized for blue response.

Inextricably linked to cathode spatial uniformity is anode uniformity. A uniform anode sensitivity is provided first and foremost by a well-designed electron-optical input system. This is especially important in linear-focused tubes in order to focus all of the emitted photoelectrons on the first dynode. In fast tubes, focusing electrodes are used to maximize collection efficiency.

The area where the sensitivity is uniform for all practical purposes is termed the useful cathode area in published data sheets. The active area however may extend to the tube wall and even onto it.

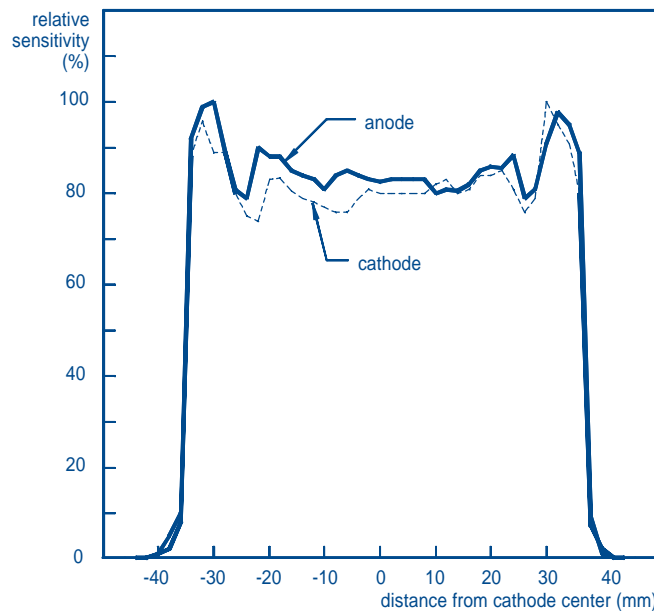


**Fig.5** Example of anode and cathode sensitivity variation measured at  $\lambda = 424$  nm along one diagonal of a XP3692, 60 mm square PMT with SbKCs cathode.

## Collection efficiency

This is a subjective parameter that is difficult to measure and for which no standardized methods have been defined. It varies considerably between PMT types, reflecting differently designed electron-optical input systems.

### Very-fast tubes

Very-fast 2" tubes such as the XP2020 are optimized for collecting photoelectrons from the whole of the photocathode surface that arrive almost simultaneously on the first dynode surface. This optimization is however at the expense of reduced collection efficiency of the available photoelectrons. This requires complex, well-optimized electron-optic designs with several input electrodes whose potentials are critical even between tubes of the same type.

### Fast tubes

Fast tubes such as the XP2262, XP4312 and XP4512 families provide a *timing-favoured* compromise between decent collection efficiency and similar photoelectron arrival times. In contrast, the XP4392 and XP4572 provide a *collection-efficiency-favoured* compromise, whilst still having very respectable timing performance. Such tubes therefore have a larger first dynode and simpler input optics than very-fast tubes.

When a good time response is required, plano-concave input windows are used to minimize geometrical path differences between the surfaces of the photocathode and first dynode.

### General-purpose tubes

Simpler still are the input optics of the general purpose tubes (Fig.7) which provide the best collection efficiency with no stringent consideration given to time response. Therefore, these tubes usually have plano-plano input windows.

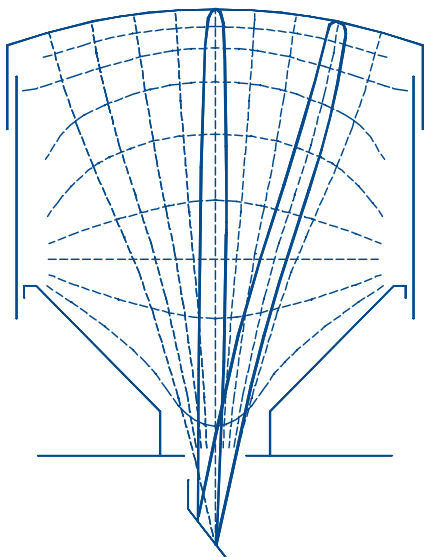


**Fig.6** Example of a large, fast PMT input electron-optics.

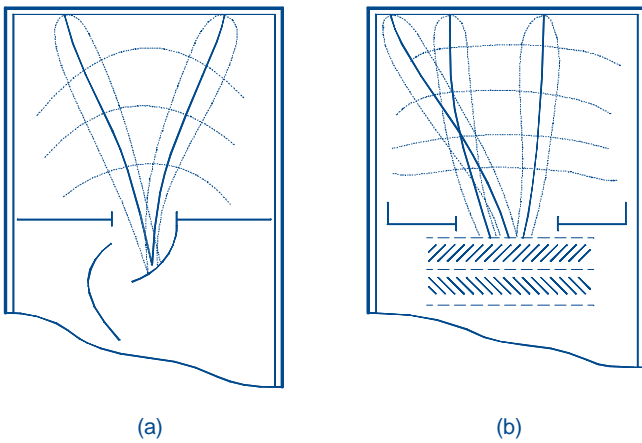


**Fig.7** Input electron-optics of a PMT with (a) focusing dynodes and (b) venetian-blind dynodes, showing equipotential lines and electron trajectories.

## Tubes optimized for PHR

Tubes optimized for the best pulse height resolution, (i.e. energy resolution) and used with the relatively slow response scintillator NaI(Tl) in gamma-camera applications, for example, are optimized for the highest collection efficiency of *all* photoelectrons - even those from the corners of hexagonal or square tubes (e.g. the XP3672 or XP3392 families), and those from the cathode on the upper part of the tube wall.

This calls for a large first dynode surface as in the box and linear-focusing multipliers of the 3" families: XP3312 (round), XP3372 (hexagonal) and XP3392 (square). PHOTONIS' low-profile tubes are another example where a large first dynode is coupled to a multiplier for optimum collection efficiency.

For instance, the XP6242 and the XP6342 families have a hybrid multiplier comprising a very large first dynode coupled to a foil multiplier. And the XP53xx family's box-and-focusing multiplier design is a linear-focusing multiplier 'folded' underneath a large first box dynode, providing an extremely short tube, sometimes termed "low-profile" tube.

Crucial between the first and second dynodes, collection efficiency is also important between the other dynodes.

## Measuring collection efficiency

To obtain reproducible relative measurements of collection efficiency for a particular PMT type, the only good method is to measure the pulse height resolution, PHR, for a known isotope energy (e.g.  $^{57}\text{Co}$ , 122 keV) with the PMT coupled to a high-quality standard-size scintillator whose relative PHR is well known and to compare the results obtained.

Pulse height resolution mainly depends on:

- scintillator quality,
- PMT quantum efficiency,
- PMT collection efficiency,
- PMT gain statistics of the first dynode,
- PMT gain statistics of subsequent multiplier stages, and resolution of the measuring circuit.

The relative collection efficiencies of tubes having the same quantum efficiency can be compared by keeping all the other parameters constant.

The literature indicates how to relate PMT collection efficiencies to a figure of merit in Cherenkov measurements, and there have been trials to define a method of measuring the absolute collection efficiency of large hemispherical PMTs. These methods are however neither practical nor common for other PMT types.

Collection efficiency comparisons can therefore best be avoided and replaced by comparisons of relative PHR under well-defined conditions that give reproducible results.

Curves, like those in Fig.5, giving the anode and cathode sensitivity measured by scanning the diagonal with a perpendicular light pencil beam typically show a higher sensitivity at the faceplate periphery. This is however due to the measurement method - light reflected from internal electrodes gives the reflected photons one more chance to strike the photocathode. Such reflexions can also occur in practice, their effect on sensitivity depending on how the photons arrive at the photocathode.

## The electron multiplier

The electron multiplier of a PMT is a virtually noiseless, high-gain, wideband amplifier for the electrons extracted from the photocathode. As already described, the electrons are multiplied by a cascade of secondary emission at several dynodes.

The main types of multiplier used in PHOTONIS PMTs, are (see Fig.8):

- **the linear-focusing** multiplier whose in-line dynodes progressively focus the electron paths through the PMT. This type of multiplier provides high gain, good timing characteristics, and high linearity.
- **the venetian-blind** multiplier with dynodes consisting of an assembly of parallel strips. This multiplier has good collection efficiency, and respectable immunity to external magnetic fields.
- **the foil** multiplier with dynodes of perforated metal foil, which are precision-designed alternatives to standard mesh dynodes. Foil dynodes provide the extremely low crosstalk utilized in the segmented tubes of the XP1422 and XP1452 families, and in the XP1700 family of multi-channel PMTs,
- **the box or box and grid** multiplier has a large collection area at the first dynode, and hence good collection efficiency, but slightly degraded timing characteristics,
- **the circular cage** multiplier leads to highly compact arrangements,

- **the microchannel plate (MCP)** multiplier consist of a microchannel-plate electron multiplier with a proximity focused cathode at one side and an anode at the other. The microchannel plate is a compact aggregation of parallel glass tubes of microscopic diameter ( $6 - 25 \mu$ ). One electron at the input is multiplied in a single microchannel. High gain is obtained by arranging two MCP in cascade (XP85002, XP85012 and XP85022).

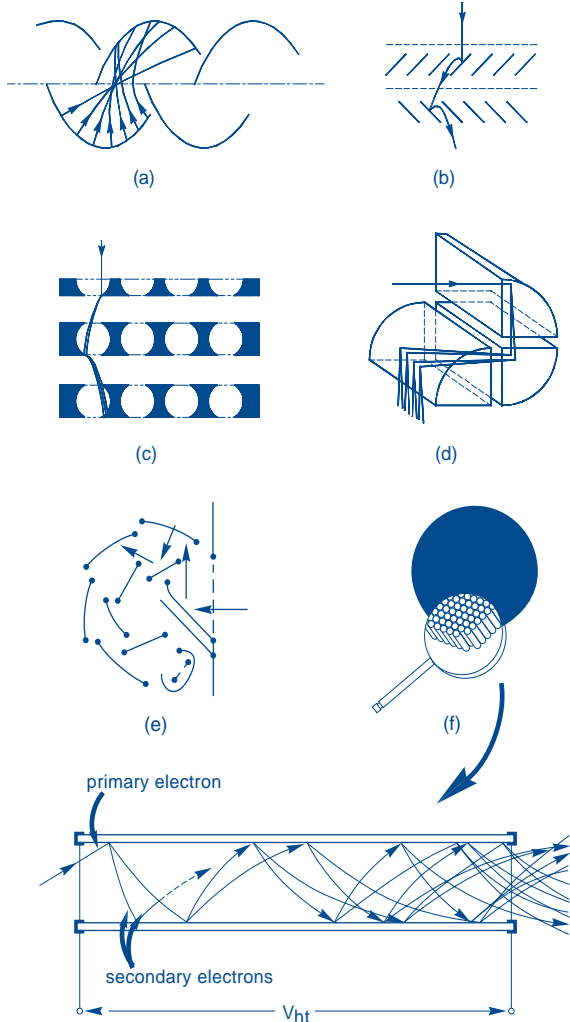


**Fig.8** Dynode configurations of electron multipliers:  
(a) linear focusing, (b) venetian blind, (c) foil, (d) box,  
(e) circular cage and (f) MCP.

Each type of multiplier reflects trade-offs between parameters such as gain, response time, collection efficiency (related to PHR) and tube length. In recent years, new hybrid multipliers have been designed to optimize these trade-offs, for example:

- the box and linear-focusing multiplier: where the collection sensitivity and magnetic immunity of a conventional linear-focusing multiplier have been enhanced by a new design of input optics and first dynode. Examples: XP3212, XP3312 and XP3392 families.
- 'low-profile' box-and-focusing multiplier: a variant of the above with 'folded' multiplier, providing a very short tube. Examples: XP5202, XP5302 and XP5612 families.
- a foil first dynode followed by a linear-focusing multiplier. Example: XP1802.
- large focusing first dynode followed by a short foil multiplier. Examples: XP6242 and XP6342 families.

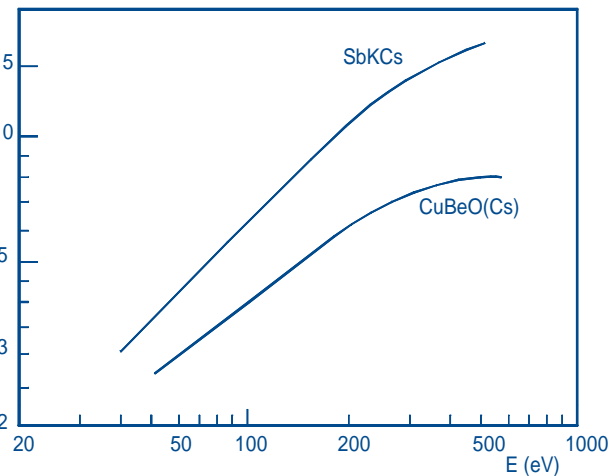


**Fig.9** Secondary emission coefficients,  $\delta$ , of the commonly used dynode materials, as functions of incident primary-electron energy,  $E$ .

## Secondary emitting dynode coatings

To form a secondary-electron emitting layer, the surfaces of the metal dynodes (usually beryllium copper) are oxidized or coated with an alkali antimonide layer.

Oxidized beryllium copper dynodes provide a superior time response and linearity due to the high multiplier voltage needed for a given gain; and better long-term stability at high operating currents. Alkali antimonide coated dynodes (of the same composition as the cathode) operate at a lower voltage for a given gain, and provide a more stable gain performance when count rates change. In addition, they have better long-term stability at low anode currents.

Moreover, in tubes with alkali antimonide coated dynodes, the voltage between the cathode and the first dynode can be higher giving a first-dynode gain reaching 10 to 20. This provides a single-electron pulse height spectrum with a well-defined peak resolution as good as 60% - a feature of fast tubes like the XP2020 and XP2262.

## Voltage dividers

The voltages required to create the electrostatic fields between dynodes to accelerate and focus the electrons in a PMT are most conveniently derived from a single high-voltage supply and a voltage divider network.

The design of the divider network is crucial to get the best performance from the PMT, but the inter-electrode voltage distribution will always be a trade-off between certain performance parameters (a high voltage between cathode and the first dynode is however always recommended). That is why we publish up to three voltage divider circuits (Fig.10) in data sheets:

- **type A:** iterative voltage distribution; the same voltage for all multiplier stages (except the first few). This distribution provides the highest gain for a given supply voltage and is particularly suitable for photometry and nuclear spectrometry applications.
- **type B:** progressive voltage distribution (increasing from the cathode to the anode). This distribution provides the highest linear peak current but with a much lower gain than type A.
- **type C:** 'intermediate' progressive voltage distribution. This distribution optimizes time characteristics while providing acceptable gain and linearity. Type C dividers are particularly suitable in physics experiments requiring accurate timing combined with ability to analyze pulse heights over a wide dynamic range.

In this catalogue, the published gain curves and gain values are given for type A dividers unless stated otherwise.

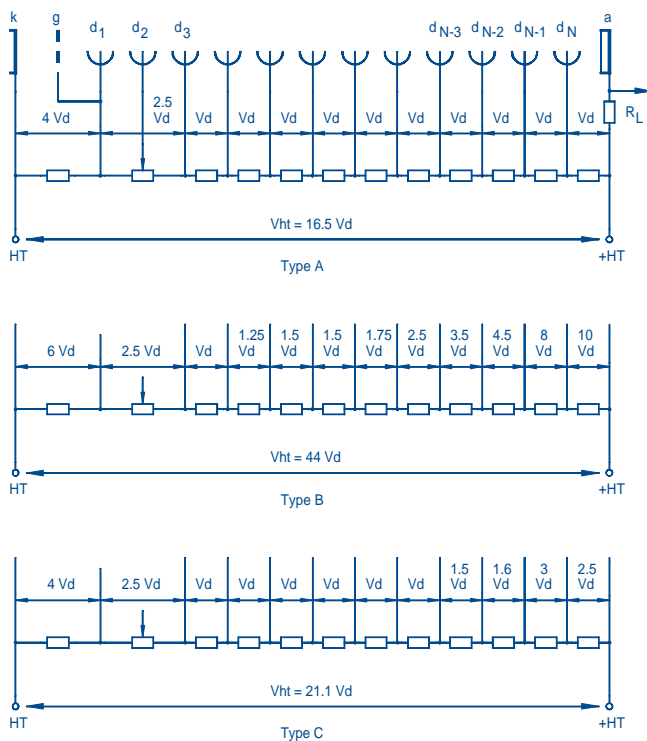


**Fig.10** Voltage dividers: type A, iterative, type B, progressive, type C, intermediate. V<sub>d</sub> is the smallest inter-dynode potential.

#### **Gain and pulse linearity of a fast response photomultiplier, with different voltage distributions**

Type of voltage distribution	Gain V <sub>ht</sub> = 2500 V	Linear within 2% for current pulse amplitudes up to
A	1.2 x 10 <sup>8</sup>	40 mA
B	0.7 x 10 <sup>6</sup>	250 mA
C	2 x 10 <sup>7</sup>	100 mA

## **Gain**

The gain or current amplification, G, of a PMT is the ratio of the anode current to the photocathode current. It varies as a power of the supply voltage (usually >5) and:

$$\frac{G_2}{G_1} = (V_2/V_1)^{\alpha N}$$

where G<sub>2</sub> and G<sub>1</sub> are the gains at supply voltages V<sub>2</sub> and V<sub>1</sub> respectively,

$\alpha$  is a coefficient (0.6 to 0.8) set by the dynode material and geometry, and N is the number of dynodes.

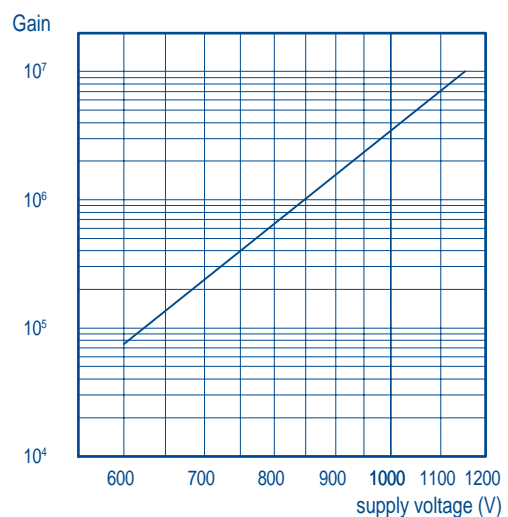


**Fig.11** Published gain curve for XP2042 tubes.

Published gain curves like that shown in Fig.11 are on log-log coordinates, and are therefore straight lines of slope  $\alpha N$ . For a given PMT type, the gain curves for different voltage dividers are parallel. Data sheets give the typical value of the slope making it easy to calculate the gain at any supply voltage (or vice versa) once the gain at one voltage is known for individual tubes.

For example, for an XP2042,  $\alpha N$  is typically 7.5, so for a 10% voltage increase, the gain will approximately double. A practical consequence of this is that the stability of the power supply has to be better than 1 part in a thousand.

## **Anode collection space**

The shape and arrangement of the electrodes at the output end of the multiplier again differ from those used in the input and iterative parts. The geometry must be suitable for:

- collecting all the secondary electrons emitted by the last dynode,
- minimizing space charge effects to ensure linear response in pulse-mode operation,
- matching the anode impedance to the characteristic impedance of the output connection.

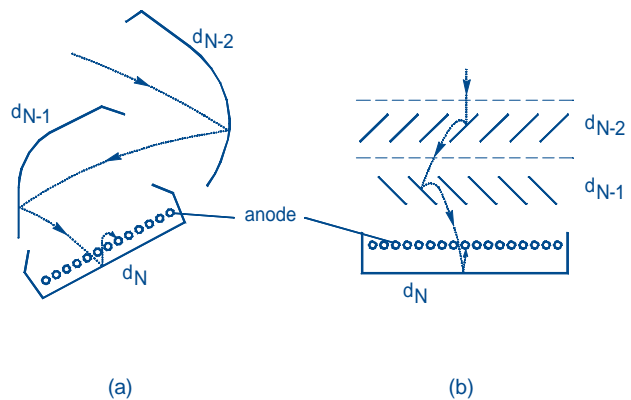


**Fig.12** Collection-space configurations: (a) with focusing dynode, (b) with venetian-blind dynodes.

Figure 12 shows the collection spaces of two general-purpose photomultipliers. The collector, or anode, is a grid positioned close to the last dynode so that secondary electrons emitted by the next-to-last dynode pass through it but those emitted by the last dynode are collected. Such a configuration makes it possible to obtain a high electric field between the last dynode and anode and so reduce the space charge effect in the last stage. Furthermore, the last dynode forms a partial electrostatic screen around the collector grid.

## Anode sensitivity

Anode sensitivity (including collection efficiency) is simply the product of cathode sensitivity, collection efficiency and gain. It varies with supply voltage exactly as gain does.

As for photocathode sensitivity, anode sensitivity can be classified into:

- **anode radiant sensitivity**, expressed in A/W at a given wavelength; used in only a few applications,
- **anode luminous sensitivity**, expressed in A/lm; PHOTONIS uses this to specify and routinely test PMTs with standard multialkali and ERMA cathodes;
- **anode CB sensitivity, or anode ‘blue’ sensitivity**, expressed in A/lmF (F for filtered); PHOTONIS uses this to specify and test all bialkali types intended for NaI(Tl) scintillation detection. There is a good correlation between blue sensitivity and the pulse height observed at the anode of a tube in response to scintillations from a given NaI(Tl) crystal.

By tradition, some fast tubes are still specified and tested for gain.

## Specifications and testing

The following method is used to measure anode sensitivity. For each PMT type, an anode sensitivity (or, where applicable, a gain) that is typical for the application is defined usually with a type A divider (e.g. 7.5 A/lmF for the XP2042,  $3 \times 10^7$  gain for the XP2020). The supply voltage is then adjusted to the exact value that provides the nominal sensitivity (or gain); the specification gives maximum and typical values to this voltage, and for each tube the corresponding supply voltage is put on the test ticket.

The gain spread in a batch of tubes can be measured by operating all the tubes at the same voltage. Note that the spread in the supply voltage ratio  $V_{max}:V_{min}$  can be 1.3:1 (and even 1.4:1) corresponding to a spread in gain ratio at a given voltage of 5:1 (and even 10:1).

## Maximum voltage ratings

Recurrent breakdown in a PMT may destroy the associated electronics and eventually the PMT itself. Therefore, the supply voltage should not exceed the specified maximum rating.

For example, it is specified in the XP2042 data sheet that this PMT should not be used above 75 A/lmF or 1400 V (independent limits). If an XP2042 test ticket indicates a supply voltage of 900 V for the *nominal* sensitivity (7.5 A/lmF), the required voltage for 75 A/lmF is (from the gain-voltage relationship  $G_2/G_1 = (V_2/V_1)^{\alpha N}$  with  $\alpha N = 7.5$  for an XP2042):  $900 \times (75/7.5)^{1/7.5} \approx 1250$  V.

which is the limit for this specimen. If the tube is used with a different type of voltage divider, the required supply voltage for 75 A/lmF sensitivity may exceed the 1400 V limit, and the tube must not be operated under these conditions.

All PHOTONIS tubes are regularly tested at maximum voltage and sensitivity to check that the dark noise is less than a preset limit, and that breakdown does not occur.

Take care that the maximum ratings of inter-electrode voltages are also not exceeded, as can occur by using an exotic divider, resulting in increased noise or breakdown. Note that data sheets also give *lower limits* for the cathode to first dynode voltage to ensure an acceptable collection efficiency, and for the last dynode to anode voltage to ensure an acceptable linearity.

## Anode dark current & dark noise

In total darkness, a photomultiplier tube still produces a small output current called anode dark current. Similar to a photoelectric current, the main component of dark current is the charge sum of several short pulses usually of the same duration as single photoelectron pulses. The rate of these pulses is called the dark noise or dark count rate (for clarity, the term background should be avoided in this context). Dark current and dark noise limit the detectivity of a PMT.

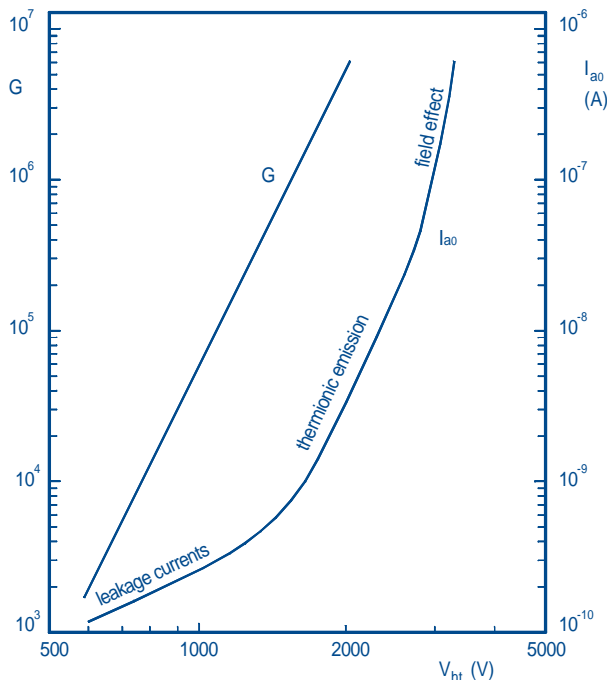


Fig.13 Gain G and anode dark current  $I_{a0}$  as functions of the PMT supply voltage, showing the voltage regions in which each of the three main causes of dark current predominates.

## Ohmic leakage

This component of dark current is due to leakage currents between electrodes on the glass and insulating surfaces of the tubes (plastic bases, sockets). It is a major part of dark current when a PMT is operated at low gain ( $<10^4$ ) or at low temperature. Dirt and humidity are obvious major contributors, but soldering flux too is particularly harmful, producing large dark noise pulses (similar to scintillations) at all values of gain.

## Thermionic emission

Thermionic emission of single electrons from the cathode is the main component of dark current, and the corresponding pulse height spectrum is the same as that for single photoelectrons.

A typical bialkali cathode emits about 50 electrons/cm<sup>2</sup>.s at room temperature; cathodes with a response extending into the infrared have a higher emission. As long as thermionic emission dominates, the dark noise is independent of supply voltage (or gain), although of course the dark current increases with gain.

Thermionic emission varies with temperature according to the Richardson law (i.e. about a ten-fold increase for a 15°C temperature rise). Thermionic emission can therefore be reduced by lowering the temperature of a PMT (0 to -25°C) provided other dark current causes do not become dominant and the resistivity increase of bialkaline cathodes can be tolerated.

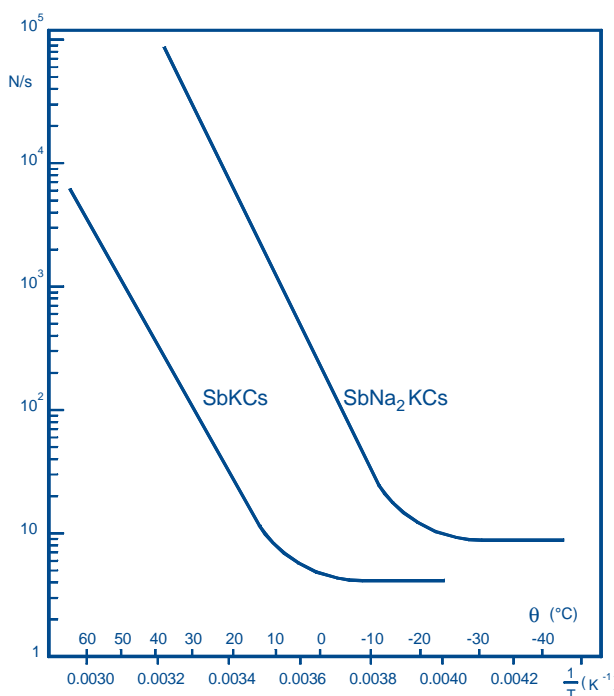


**Fig.14** Number of dark pulses per second as a function of temperature for SbKCs and SbNa<sub>2</sub>KCs photocathodes.

## Field emission

Local electric fields in a PMT can be very high, and any blemish on an electrode, or a loose particle can be a potential source of field emission, also known as cold emission. Electrons emitted by field emission are accelerated onto other surfaces inside the tube and, even those with just 1 keV energy, may be able to extract more (photo)electrons from the cathode and dynode surfaces.

Field emission increases more rapidly with supply voltage than gain does, and the dark current soon becomes unstable and erratic. The pulse height spectrum of such dark noise always contains more large (multielectron) pulses than the normal single-electron spectrum, and also many small pulses below 0.2 PE (photoelectron) equivalent that originate from the first dynodes. These small pulses can also appear as fast bursts.

All PHOTONIS PMTs are tested at maximum supply voltage ratings to ensure field emission is at acceptable levels. Nevertheless, when dark noise is critical, it is recommended to operate a PMT well below the maximum voltage rating.

To minimize the risk of field emission, some high-gain tubes have an external conductive coating connected to the cathode.

## Radioactivity

All glass windows, bulbs as well as internal parts contain traces of natural radioactive isotopes like <sup>40</sup>K, <sup>232</sup>Th, <sup>238</sup>U. The natural decay of these elements as well as those of the decay chain can produce scintillations in the glass itself or in the scintillator to which the PMT is coupled.

Depending on the application, there may be a need for low

radioactivity glass for the window or even sometimes the entire glass bulb as well as the internal tube parts.

For each of these, the gamma emission per decay can be calculated over an energy spectrum. For example, Thorium emits 4.14 gamma per decay with 2.74 above 0.1 MeV per chain.

The relation between the concentration of the element in the glass called C in ppb and the activity A in Bq/kg is:

$$C \text{ (ppb)} \approx 75.6 \times 10^{-12} \times A \times N \times T$$

where

A is the atomic mass of the element in g,

T is the half-life period of the element in years.

Our new low radioactivity glass is down by a factor 30 compared to a standard low noise borosilicate glass in term of decay per second. It means that a glass window of 2mm thickness that used to generate 180 cpm (count per minute) is now down to 4 cpm for our XP3xK0 family tube (2", 3", 3<sup>1/2</sup>", 5").

## PMT without scintillator

When a PMT is used without a scintillator (e.g. in photon counting), or with a small scintillator, the major effect is due to β particles (from <sup>40</sup>K) emitted inside the glass window and reabsorbed within 1 mm, producing light pulses by Cherenkov radiation. The anode pulse height spectrum of such pulses extends from 1 to 20 PE, but the rate rarely exceeds 10 or 20 counts/s even with a high potassium content window (as opposed to 50 to 5000 counts/s for thermionic emission). Beta particles become a problem when the pulse height range of interest is above 5 PE, or in coincidence measurements. In photon counting, most of them can be eliminated from the measurements by using an upper counting threshold of 3 to 5 PE.

High-energy particles from cosmic ray showers can also produce pulses in the window of up to 100 PE or more, but the rate is very low.

## PMT with scintillator

When a PMT is used with a large scintillator, the gamma rays emitted by the same isotope traces in the complete PMT glass bulb (not only in the window) are the source of unwanted scintillations.

## Cathode excitation

When a tube is exposed to even very low levels of ambient light, especially just before the tube is put into operation, the dark current in operation can initially be several orders of magnitude larger than that when the tube has stabilized several hours or even days in darkness.

The pulse height spectrum is similar to that for single photoelectrons. This phenomenon is very dependent on the cathode substrate. In normal use, take simple precautions to limit exposure. In all cases, avoid fluorescent light and daylight.

## Dark current values on test tickets

All PHOTONIS PMTs are factory-tested for dark current. For each specimen, an individual dark current or dark noise value at nominal sensitivity is usually printed on the test ticket. This value should be considered as the maximum that could be observed after stabilization in darkness.

Tubes whose PHR is tested using a <sup>55</sup>Fe or <sup>57</sup>Co source don't have dark current values listed on the test ticket. This is simply because these tubes passed a much more stringent dark noise test during the measurement of their PHR, listed on the test ticket.

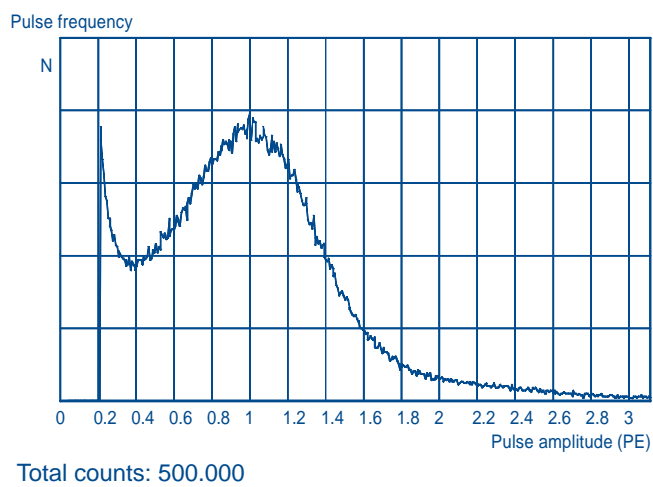


**Fig.15** Example of dark-current spectrum with linear focused dynodes. (XP2960 tube).

## Afterpulses

Afterpulses are spurious pulses that appear in the wake of true pulses. They can be observed on an oscilloscope while detecting very short flashes such as scintillation and laser pulses. As they are time-correlated with the true pulses, they are particularly inconvenient in chronometry and time spectrometry applications using coincidence techniques; in counting applications they often spuriously limit the number of true pulses that can be registered.

Afterpulses have two main causes:

- luminous reactions (that is, light emitted by electrodes due to electron bombardment),
- ionization of residual gas traces.

They can be distinguished by the interval that separates the afterpulse from the true pulse.

The effects of afterpulses can be minimized by using coincidence techniques, by blanking the photomultiplier for a set interval after each true pulse, or simply by using measuring equipment with sufficiently long dead time.

In Cherenkov telescopes viewing high photon rates from the night sky, afterpulse rates can nevertheless be considerable. This is why we have designed tubes like the XP3062 and XP2960, specially manufactured to minimize afterpulse effects.

### Afterpulse durations

afterpulse source	duration (typ.)
luminous reactions	20 to 100 ns
ionization of residual gases:	
- in the electron-optical input system	$\text{H}_2^+$ : 0.3 $\mu\text{s}$ $\text{He}^+$ : 0.4 $\mu\text{s}$
	$\text{CH}_4^+$ : 1 $\mu\text{s}$
- in the electron multiplier	1 to several $\mu\text{s}$ , e.g. 3 $\mu\text{s}$ for $\text{Cs}^+$

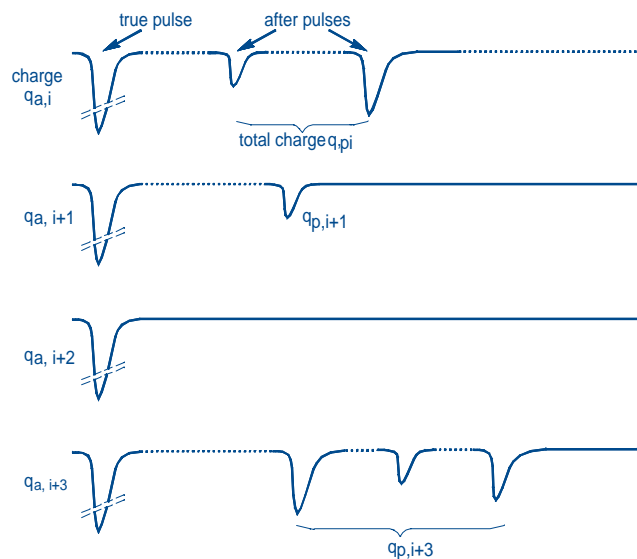


**Fig.16** Examples of the development in number and charge of afterpulses.  $q_{a,i}$  etc. is charge transferred by true pulses;  $q_{p,i}$  etc. that transferred by afterpulses.

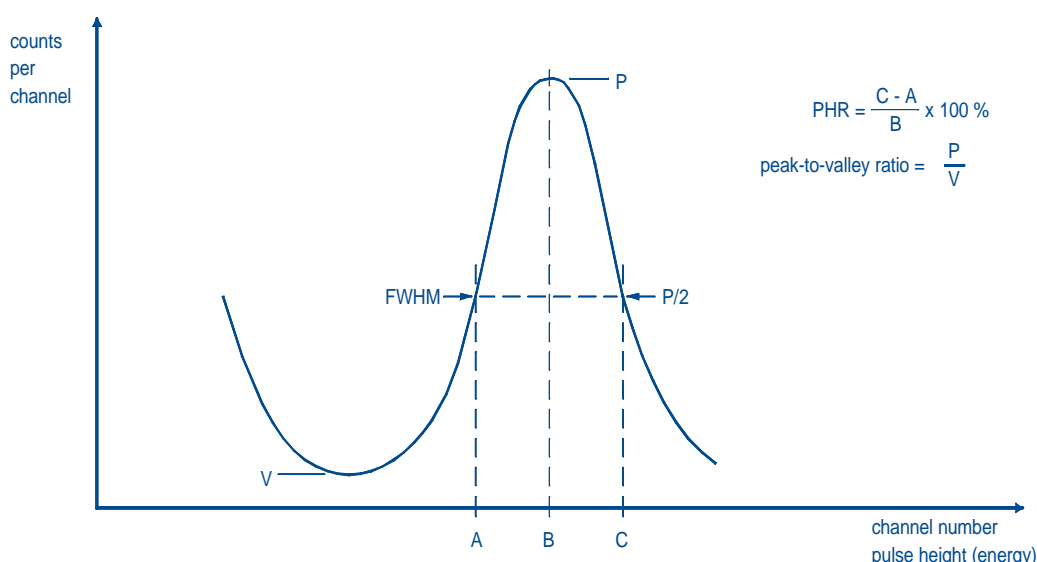


**Fig.17** Typical pulse height spectrum showing the definition of pulse height resolution and peak-to-valley ratio.

## ■ Figures of merit

Although the electron multiplier of a PMT is virtually noiseless, signal extraction from the noise has still to be considered carefully. This, and statistical fluctuations of the anode current lead to three main figures of merit for different applications:

- pulse height resolution for pulsed operation (e.g. in scintillation counting),
- single-electron resolution for single-electron counting,
- signal-to-noise ratio for continuous operation (e.g. in a flying-spot scanner).

### Energy spectrum and pulse height resolution (PHR)

Figure 18 shows a well-known type of energy spectrometer using a multi-channel pulse-height analyser. Each scintillation gives rise to an anode charge  $q_{a,s}$  proportional to the energy deposited in the scintillation process. The charge amplifier converts the charge into a proportional voltage pulse which is amplified and fed into the analyser. As successive pulses occur, the analyser constructs a histogram of their amplitudes  $u_q$ , see Fig.17, called the pulse height spectrum, or energy spectrum since the pulse heights are proportional to the energy of each of the  $\gamma$  quanta incident on the scintillator.

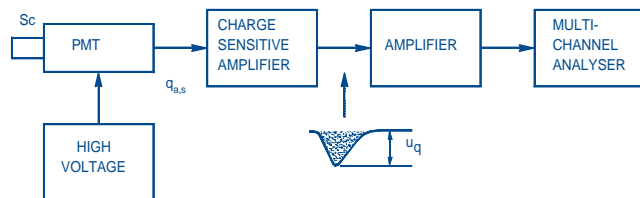


**Fig.18** Energy spectrometer using a multichannel pulse-height analyser.

The energy resolution, or pulse height resolution (PHR) for a specified radioactive decay is given by:

$$\text{PHR} = \frac{\text{FWHM}}{\text{peak}} \times 100\%$$

The better the resolution, the greater is the peak-to-valley ratio (Fig.17).

Our published values for PHR are obtained using standard high-quality scintillators, making PHR dependent mainly on the PMT performance. This enables relative comparisons to be made between tubes.

### Single-electron resolution (SER)

At very low light levels, single photoelectrons can produce individual output pulses within the response time of a PMT. The rate of these pulses is a measure of the light intensity. It is usual however to measure and sort these pulses in a similar way to that used to construct the pulse height spectrum, (only now the illumination is so low that each voltage pulse has a very low probability of being due to the emission of more than one electron at the photocathode.) The resulting anode pulse histogram obtained from a multi-channel analyser is the single-electron spectrum. The single-electron resolution being defined as for the pulse height resolution.

A high-gain first dynode is required for good SER.

### Signal-to-noise ratio

This figure of merit is important when a PMT is used in continuous mode (for example, in a flying-spot scanner) where the cathode photocurrent fluctuates randomly about a mean value. This phenomenon is referred to as statistical shot noise, and its influence on signal-to-noise ratio is described in depth in the Photonis application book.

## ■ Timing

### Response pulse width

This is defined as the full width at half maximum (FWHM) of the anode current pulse delivered in response to a delta-function light pulse (Fig.19(a) and 20). Although it is not practicable to generate true delta-function light pulses, it is practicable to generate light pulses whose FWHM is much less than that to be measured.

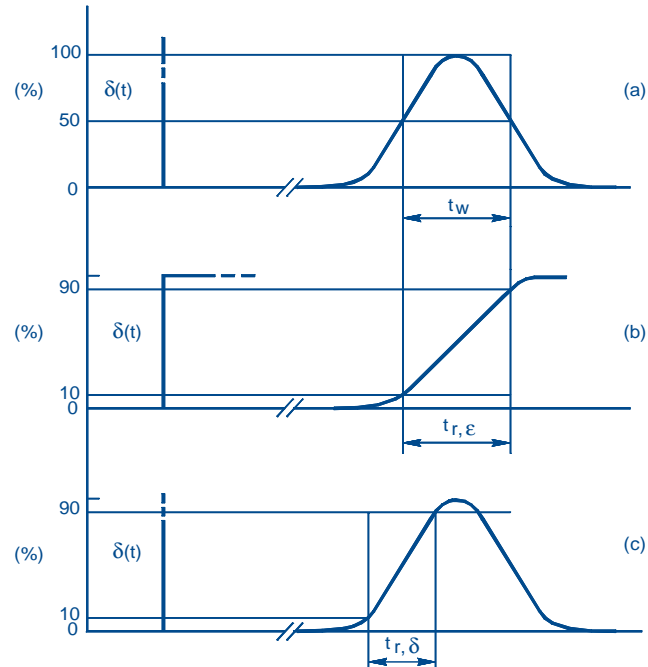


**Fig.19**  
(a) delta-function input response-pulse width  $t_w$   
(b) step-function input response rise time  $t_{r,\epsilon}$   
(c) delta-function input response rise time  $t_{r,\delta}$ .

If the pulse response width is more than a few nanoseconds, it can be satisfactorily measured using light pulses of 1 ns FWHM. Modern lasers are capable of generating light pulses with a FWHM of <100 ps. Such lasers are expensive, however, and are usually only found in advanced measuring systems.

### Rise time

Step-response rise time is properly defined as the time required for the anode current to increase from 10% to 90% of its final value in response to a unit step input. Measured under these conditions, the rise time approximately equals the response-pulse width for a delta function light (Fig.19(b)).

However, owing to the difficulty of producing unit steps of light, the rise time is by convention defined as the 10% to 90% rise time of the anode current pulse in response to a light pulse that approximates a delta function (Fig.19(c)). It varies from about 1.5 ns for photomultipliers with linear-focusing dynodes to about 15 ns for those with venetian-blind dynodes.

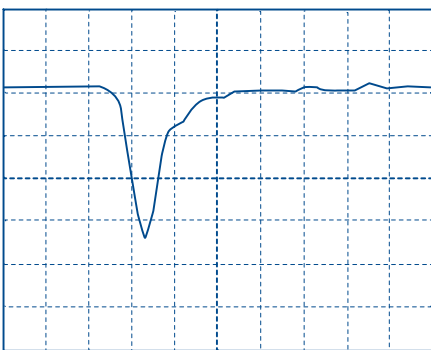


**Fig.20** Anode pulse response of a fast-response PMT. Vertical scale, 100 mV/div Horizontal scale, 5 ns/div.

## Transit-time and transit-time differences

The interval between the arrival of a light pulse at the cathode and that of the corresponding current pulse at the anode is called the transit time. Its mean value evaluated over a statistically large number of pulses, varies as  $1/\sqrt{n_{ht}}$  and is usually of the order of several tens of nanoseconds.

In general, the mean transit time differs according to where on its surface the cathode is illuminated. When measured with reference to one point of illumination at the centre of the cathode and another at the edge, the corresponding *transit-time difference*  $\Delta_{CE}$  is called the *centre-edge difference*.

## Transit-time spread, time resolution

Transit-time fluctuations from light pulse to light pulse are observed when identical pulses strike the same part of the cathode (Fig.21).

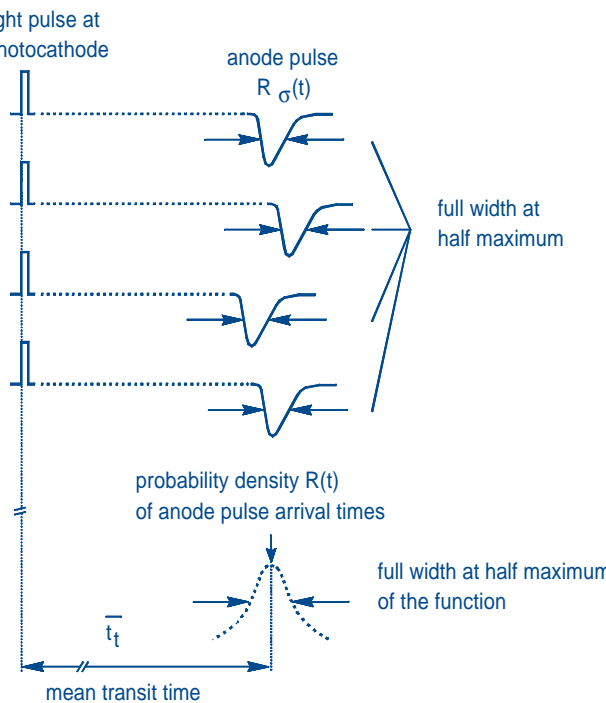


**Fig.21** Response-pulse jitter due to transit-time fluctuations.

The *transit-time spread* (also called *jitter*, or *time resolution*) is defined as the FWHM of the probability distribution of the fluctuations. It is practically proportional to  $1/\sqrt{n_k}$  where  $n_k$  is the number of photoelectrons per pulse. Like the transit-time differences, the time resolution depends on the size and location of the illuminated part of the cathode; it also depends

on the voltage applied to the electron-optical input system and on the spectral character of the illumination.

PHOTONIS specifies transit-time spread in terms of the standard deviation  $\sigma$  of the probability distribution of the transit-time fluctuations. It is a worst-case value based on single-photoelectron pulses originating from points distributed over the *whole* surface of the cathode ('open cathode'), i.e. including the centre-edge difference as defined in IEC standards. FWHM values are  $\approx 2.34\sigma$ .

How the time characteristics of a photomultiplier depend on the different parts of the tube, such as the input system, the multiplier, and the anode collection space, is covered in Chapter 4 in the Photonis application book.

### Typical time response of some 'fast' tubes in single-electron mode

PMT type	$t_r$ (ns)	$t_w$ (ns)	$\Delta_{CE}$ (ns)	transit-time spread, $\sigma$ (ns)	divider / HT
XP1911	2.4	3.8	1.5	1.0	B / 1700 V
XP2020	1.5	2.4	0.25	0.25	C / 2500 V
XP2020/UR <sup>+</sup>	1.4	2.3	0.15	0.15	C / 3000 V
XP2262	2.0	3.0	0.7	0.5	B / 2300 V
XP2282	1.5	2.2	0.5	0.4	C / 2500 V
XP4312	2.1	3.3	0.5	0.4	C / 2500 V
XP4512*	2.1	3.0	0.8	0.6	B / 1700 V

$t_r$ : anode pulse rise time (10%-90%);

$t_w$ : anode pulse width (FWHM);

$\Delta_{CE}$ : center-edge transit-time difference;

$\sigma$ : transit time spread measured for an open photocathode.

<sup>+</sup>: M. Moszynski, *Prospects for new fast photomultipliers*,

NIM A337 (1993) pp.154-164.

<sup>\*</sup>: M. Moszynski et al., NIM A307 (1991) pp.97-109.

## ■ Linearity

The ratio of the number of incident photons to the number of electrons collected at the anode is called *charge linearity*. The proportionality between incident flux and anode current is called *current linearity*; in this relationship therefore, *time* is an additional parameter. Limits on both charge and current linearity are set by internal and external factors. PHOTONIS' PMTs meet the highest linearity demands and have an excellent large dynamic range.

## External factors affecting linearity

### Power supply

Changes in inter-electrode voltages affect gain by influencing the dynode secondary emission factors and the electron trajectories.

### Divider current

When the electrode voltages are derived from a resistive divider across a stabilized power supply, the anode current,  $I_a$ , tends to lessen the potential between the last dynode and the anode. This upsets the voltage distribution throughout the divider and causes an increase of gain comparable to what would be caused by increasing the high voltage by the same amount.

With a divider current  $I_d$  (at  $I_a = 0$ ), the gain change is:

$$\frac{\Delta G}{G} \approx \frac{\alpha N I_a}{N+1 I_d}$$

where  $\alpha$  is the exponent of gain variation (0.6 to 0.8),  $N$  is the number of dynodes and  $I_a$  the actual anode current.

Provided the decrease of voltage across the terminals of the last stage does not impair collection efficiency, the ratio  $\Delta G/G$  has the same sign as  $I_a/I_d$ : an increase of  $I_a$  results in an increase of gain (Fig.22). This increase (or overlinearity) as a function of  $I_a$  is largely independent of  $N$ . For  $\alpha = 0.7$ ,  $N = 10$ , and  $I_a/I_d = 0.1$ , it amounts to about 7%.

When the ratio  $I_a/I_d$  approaches unity, the expression for gain change no longer holds. The voltage drop in the last stage, which increases with  $I_a$ , becomes too great and collection efficiency declines rapidly, leading to an abrupt decrease of gain (Fig.22).

The maximum value of the ratio  $\Delta G/G$  mainly depends on the voltage across the tube and how the drop between anode and last dynode affects the voltage distribution among the first stages.

The dependence of gain on anode current can be optimised using transistorized dividers, see Fig 31 (p.24).

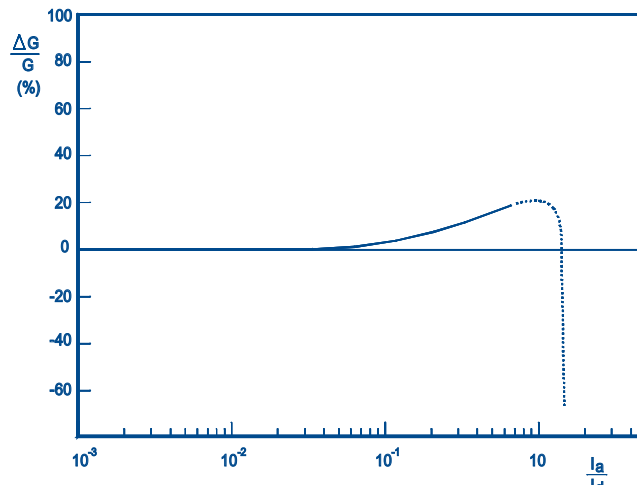


Fig.22 Gain variation (overlinearity) as a function of the ratio  $I_a/I_d$ .

### Reservoir capacitors

When the anode current can reach high values for only a small fraction of the time (short-pulse operation), it is preferable to connect reservoir (or decoupling) capacitors to the dynodes. The charge stored by the capacitors must be sufficiently large compared with that supplied by each dynode when pulses pass through the tube so that the dynode potentials will not vary by more than one or two volts. Calculation of the required capacitance values differs according to whether the decoupling is parallel or series; in the latter case voltage variations are cumulative. For a capacitance calculation example, see Supply and Voltage Dividers.

### Damping resistors

When a photomultiplier is operating in pulse mode, a high-frequency spurious oscillation superimposed on the anode pulses ("ringing") may be observed, even with pulses as wide as a few hundred nanoseconds. This oscillation, which affects the linearity characteristic of the tube, usually producing an overlinearity, may appear abruptly when the anode current exceeds a certain level. One way of overcoming this effect is to connect a  $50\Omega$  non-inductive resistor in series with each of the last two or three dynodes. Fast-response photomultipliers with plastic bases have such resistors built-in. For other types

they must be wired into the socket, between the base and the decoupling capacitors.

### Anode load

The voltage developed across the anode load subtracts from the last-dynode to anode voltage and, if it is not negligible compared with that, may affect linearity. As the load voltage rarely exceeds a few volts, however, this is seldom the case.

## Internal factors affecting linearity

### Space charge

At high currents, space charge can influence the electron trajectories, causing collection losses; at still higher currents it can cause some electrons to return to the surfaces from which they originate.

The current density is normally highest between the last dynode and the anode. To ensure a high field there, the anode is positioned close to the surface of the last dynode and made in the form of a grid through which the electrons pass on their way from the next-to-last dynode. Then, it is the field between the next-to-last dynode and the anode, which is 3 to 5 times lower, that sets the limit for current linearity in most photomultipliers, see Fig.12. That limit can be raised by using a progressive instead of an equal voltage distribution in the last stage so as to raise the voltage between the last two stages to as much as 300 V or more. To maintain correct focusing between dynodes without unduly increasing the gain, the inter-electrode voltages are progressively decreased in the anode to cathode direction so that the nominal value applies at the terminals of the first stages.

For tubes with focusing dynodes, the data sheets give, in addition to the conventional voltage distribution, one or two examples of recommended progressive distributions. Using these, the maximum pulse current in linear operation can be increased from 10 - 50 mA to 100 - 300 mA.

For tubes with venetian-blind or foil dynodes, the maximum pulse currents for linear operation are smaller (10 - 50 mA) because of the very low electric fields between all dynodes other than the last.

For most tubes, the current linearity limit due to space charge varies as  $V_{ht}^{-n}$ , where  $n$  is between 2 and 3. This is merely approximate, but when the limit at one voltage is known from the published data it gives a practical indication of the limit at another voltage, especially if the onset of saturation is progressive. If linearity is not important, the maximum anode current that can be obtained before saturation is several times greater than the maximum for linear operation.

The space charge phenomena that limit current linearity exist for times comparable to the transit times between dynodes, that is, 1 to 2 ns. Even when linearity errors are severe, there is no charge accumulation and the errors are strictly related to the electron current passing between the last dynodes.

Current linearity is important when pulses are wide compared with the pulse response of the tube; when they are of the same order as the pulse response, it is no longer relevant. The significant parameter then is charge linearity. Depending on the shape of the pulses, higher peak anode currents, can be obtained under short-pulse conditions while still maintaining good charge linearity.

Data sheets specify only the current linearity limit, not the charge linearity limit, and for a worst-case situation with anode pulses about 100 ns wide.

## Cathode resistivity

The electron-optical input system is designed on the assumption that the cathode is an equipotential surface. Any departure from that condition is likely to alter the electron trajectories and affect the collection efficiency of the first dynode. This is what can happen, at least in the case of semitransparent bialkali cathodes having no underlying conductive layer, when the cathode current is too large in relation to the surface resistivity. For example, a tube with a 45 mm diameter bialkali cathode exhibits a non-linearity of a few percent at a mean cathode current of about 10 nA at ambient temperature; at -30°C the same non-linearity occurs at a current of only 0.1 nA. In tubes with larger cathode diameters, the currents at which comparable non-linearity occurs are even lower.

Fortunately, the distributed capacitance of the cathode (about 1 pF) is sufficient to store a charge of about  $10^{-12}$  C. At a gain of  $10^5$ , this corresponds to an anode pulse of 100 mA amplitude and 1  $\mu$ s duration; cases in which cathode resistivity actually presents a problem are therefore fairly uncommon.

## Gain drift

Gain may undergo more or less reversible variations when the mean anode current varies. Although this too constitutes a linearity error, by convention it is treated as an instability.

## Linearity measurement

Many methods of linearity measurement have been developed but all are limited to an accuracy no better than 2%. Two types of gain drift may interfere with the measurement (see next section):

- long-term, time-dependent drift,
- short-term shift due to changes of illumination.

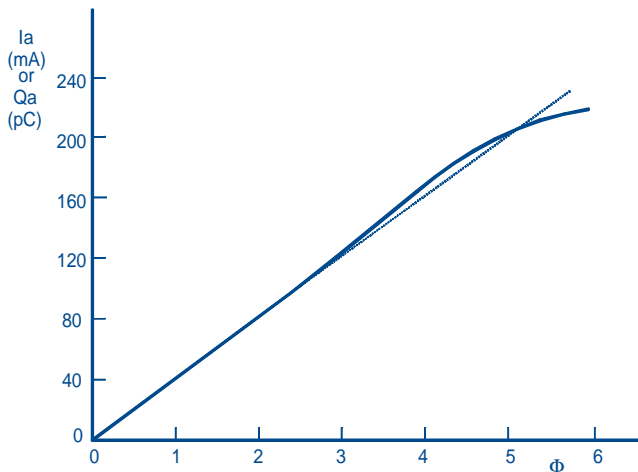


**Fig.23** Typical current or charge linearity characteristics of a PMT operating from a supply with type B voltage division (photon flux  $\Phi$  in arbitrary units).

To avoid these, the measurement must be made quickly and with a constant mean anode current not exceeding a few microamperes. The measurement should result in determining the anode current at which space charge limiting starts to become evident, avoiding all other causes of linearity limiting.

Figure 23 shows a typical linearity curve, in which a slight overlinearity appears before saturation. Such overlinearity is often observed with voltage dividers designed for delaying the

onset of saturation at high current levels. It can be corrected by adjusting the voltages of the stages immediately preceding the last, but at the cost of lowering the current threshold beyond which saturation occurs.

Several methods to measure linearity are described in the Photonis application book.

## ■ Stability

The term stability is used to describe the relative constancy of anode sensitivity with time, temperature, mean current, etc. The most important departures from constancy are:

- **long-term drift**, which is a time-dependent variation of gain under conditions of constant illumination,
- **short-term shift**, which is a variation of gain following a change in mean current.

### Long-term drift

Two modes of long-term drift can be distinguished, according to whether the mean anode current is high or low.

### High-current drift; operating life

Certain more or less irreversible effects are observable at mean anode currents larger than about 10  $\mu$ A. After long storage (e.g. a few months), a photomultiplier exhibits a large drift of gain for the first one or two days of operation. For some thousands of hours after that the gain is relatively stable, then it slowly decreases as a function of the total charge handled, Fig.24. The rate of these variations varies roughly as the anode current of the tube.

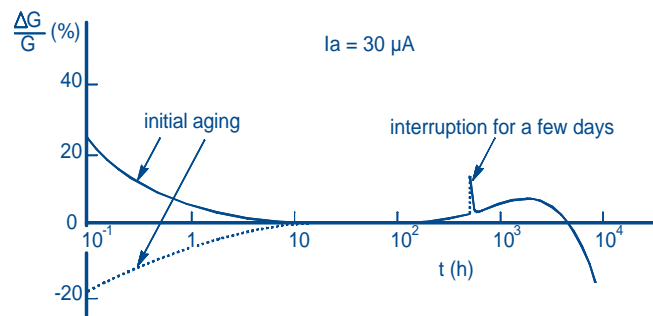


**Fig.24** Relative gain variation of a PMT operating at high average current.

Operating life, defined as the time required for anode sensitivity to be halved, appears to be a function of the total charge delivered. Values of 300 to 1000 coulombs are typical. For an XP2012, this means e.g. 30  $\mu$ A for 5000 h. If the incident flux is reduced (by, say, 90%) or cut off completely, or if the supply voltage is switched off for several days, the following sequence can be observed when the original operating conditions are restored: first, a certain recovery of sensitivity accompanied by a renewed initial drift; then, a tendency to catch up fairly quickly with the slow decline of sensitivity at the point at which it was interrupted.

Figure 24 illustrates the relative gain variation of a photomultiplier operating at a mean anode current of 30  $\mu$ A. The initial drift, which can be considered an ageing period, is between 20% and 40%. The duration of the ageing period depends on the anode current; at 10  $\mu$ A it is about 24 hours. As long as the mean current does not fall below about 100 nA, ageing is still observable though very slow.

In most cases, if the gain is high and the cathode current low, the variations of anode sensitivity reflect variations of gain due to changes in the surface state of the dynodes.

When the mean anode current is only a few microamperes, total charge delivered is no longer the decisive factor for operating life. Other effects, such as helium migration through the glass or internal migration and diffusion balances, determine the end of useful life, which is then measured in years and is independent of the mode of operation.

The experience of many users indicates that continuous, uninterrupted operation results in better long-term stability of performance characteristics than storage.

### Low-current drift

When a photomultiplier is switched on and subjected to more or less constant illumination, its gain changes over the first few hours or days (Fig.25). The amount of change differs from type to type and even from one specimen to another of the same type. In most cases, though, the rate of change quickly decreases to a few per cent a month, and the higher the current the quicker the gain stabilizes. It is sometimes worthwhile to speed the process by operating the tube initially at a current up to ten times higher than that expected in the intended application. It is also advisable to leave the tube switched on even when it is idle.

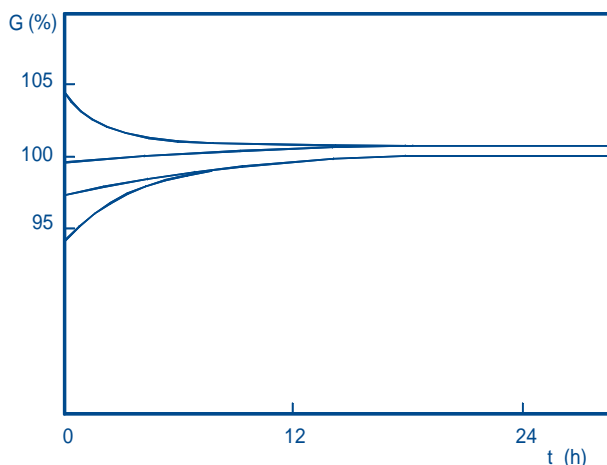


**Fig.25** Examples of initial low-current drift.

PHOTONIS uses a widely recognized ANSI (American National Standards Institute N42.9-1972) test to characterize this type of drift. The test employs a scintillator and a  $^{137}\text{Cs}$  source positioned so as to produce a fixed count rate between  $10^3$  and  $10^4$  per second. After a stabilization period of 30 to 60 minutes, the height of the  $^{137}\text{Cs}$  peak (662 keV) is recorded every hour for the next 16 hours and the mean gain deviation (MGD) calculated from:

$$\text{MGD} \approx \frac{\sum_{i=1}^{17} (p_i - \bar{p})}{17} \cdot \frac{100}{\bar{p}}$$

where  $\bar{p}$  is the mean height of the peak averaged over the 17 readings and  $p_i$  the height corresponding to the  $i$  th measurement.

This type of drift is not related to the high-current long-term drift previously described. Though its major cause is also related to change in the structure of the emissive surfaces, other factors, such as the charge distribution at insulator surfaces (e.g. dynode spacers), may also play an important part. The MGD is <1.5% for all Photonis PMTs.

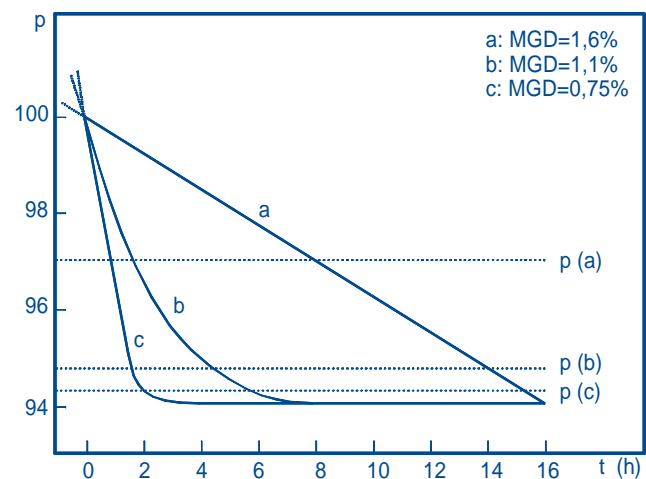


**Fig.26** Anode sensitivity curves showing the same absolute change over 16 hours but different values of mean gain deviation (MGD) according to the ANSI method ( $p(a)$ ,  $p(b)$  and  $p(c)$  are the corresponding mean heights of the pulse peak average over 17 readings).

The ANSI test specification does not mention the anode sensitivity at which the test is to be performed. However, when a figure for long term stability is given, the mean anode current during the test must be specified. For convenience, the scintillator and source used in the ANSI test may be replaced by an LED. The low-current drift over 16 hours given in the product range tables is for an anode current of 0.3  $\mu\text{A}$ .

Figure 26 gives some examples of anode sensitivity variation curves having the same maximum deviation but different MGD values.

For some applications, one may want to know the stability over a long period (for example, a month). It is possible to determine an MGD over such a period, but the measurement is more difficult because of the likelihood of drift in the measuring system itself. For such measurements, a radioactive source in combination with a scintillator is preferable to an LED because its long-term stability is much better.

### Short-term shift (or count rate stability)

When the flux to which a photomultiplier is exposed gives rise to a mean anode current of less than 10  $\mu\text{A}$ , the gain is usually sufficiently stabilized after about 10 or 15 minutes for its long-term drift to be disregarded. If the flux is then changed abruptly, the anode current, instead of assuming a new value abruptly, starts a new drift phase before stabilizing again (Fig.27).

Thus, the gain becomes a function (often an increasing one) of the mean value of the anode current reckoned over an interval of a second or longer.

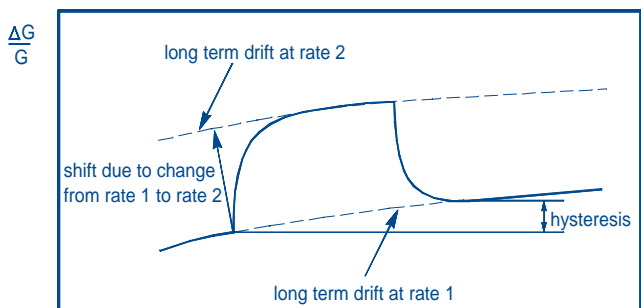


**Fig.27** Long-term gain drift and short-term shift due to change of operating conditions.

The gain shift due to a change of average flux is also measured according to an ANSI test using a  $^{137}\text{Cs}$  radioactive source and NaI(Tl) scintillator.

After a stabilization time of at least 15 minutes, the position (channel number) of the  $^{137}\text{Cs}$  absorption peak is recorded at a count rate of  $10^4$  per second. The source is then moved to reduce the rate to  $10^3$  counts per second and the new position of the peak is recorded. The shift is characterized by the relative shift of the peak.

To take account of typical photomultiplier applications, the test is usually performed between 300 nA (at  $10^4$  counts per second) and 30 nA (at  $10^3$  counts per second), or between 1  $\mu\text{A}$  and 100 nA, the value used in PHOTONIS data sheets or given on test tickets.

Tubes with bialkali cathodes and CuBe venetian-blind or SbCs coated dynodes are usually considered the most stable in respect of shift, gain variations of less than 1% being common for anode current variations of ten to one (from 1  $\mu\text{A}$  to 100 nA).

## Supply and voltage dividers

Correct use of a photomultiplier calls for observance of certain rules and circuit techniques. Those described here are indicative of present-day practice and sufficient to serve as a working guide. More detailed treatment of specific points is given in the Photonis application book.

### Applying the voltage

#### Polarity

There are two ways of applying the high voltage to a photomultiplier:

- **positive polarity**, with the cathode earthed and the anode at high positive potential (Fig.28);
- **negative polarity**, with the anode earthed and the cathode at high negative potential (Fig.29).

The choice depends on the application.

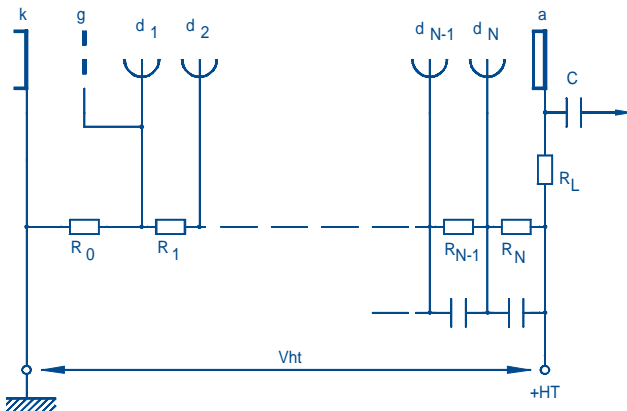


**Fig.28** Positive-polarity voltage supply.

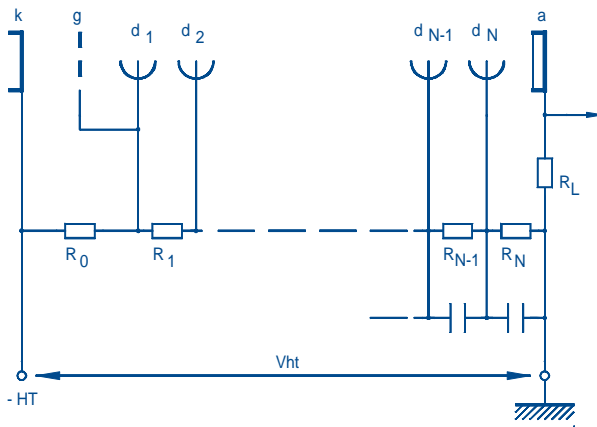


**Fig.29** Negative-polarity voltage supply.

For pulse counting, positive polarity is usually preferred; the capacitor  $C$  isolates the measuring circuits from the high voltage. Positive polarity is convenient because it does not necessitate insulating the tube from its surroundings. Magnetic screens and the coatings of scintillators should, however, be held at photocathode (earth) potential.

For applications involving detection of continuous flux or very brief pulses, where use of a coupling capacitor would be unpractical, negative polarity has to be used. This necessitates special precautions to minimize its effect on dark current and to guard the tube against the potentially destructive effect of voltage gradients across the glass (electrolysis effect).

#### Rate of voltage application

**Positive polarity.** If the high voltage is applied abruptly to a photomultiplier connected in positive polarity (Fig.31), an initial pulse of amplitude  $V_{ht} R_E / (R_L + R_E)$  is coupled through the capacitor to the preamplifier input and may cause damage. To avoid this it is advisable to use a decoupling network (shown dotted in Fig.30) with a time constant  $R_t C_t$  of at least one second. An alternative is to shunt a protection diode across the resistor  $R_E$  to eliminate all positive-going pulses at the preamplifier input.

**Negative polarity.** If voltage is applied abruptly to a tube connected in negative polarity, the amplitude of the initial dark-current transient may be high enough to damage sensitive measuring apparatus. Applying the voltage gradually reduces the transient or may even eliminate it. The RC time constant should be a few seconds.

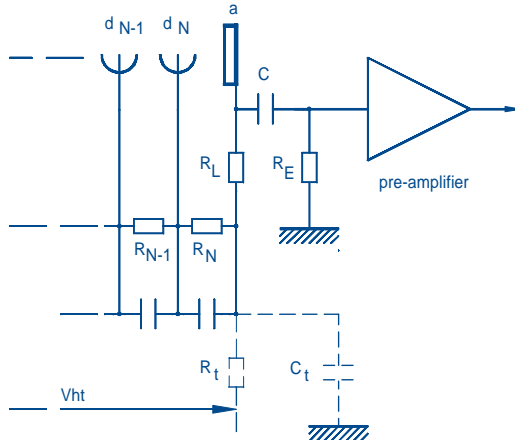


**Fig.30** Network for decoupling the high-voltage switch-on transient from the amplifier input.

## Voltage dividers

The choice of voltage divider, including the type of voltage distribution, depends on:

- **how the tube is operated;**  
e.g. continuous, pulse or high-current operation,
- **the performance required;**  
e.g. gain, linearity, timing, stability.

Besides supplying a standard range of voltage divider base sockets, PHOTONIS can provide application support to assist with the design of special divider circuitry.

## Voltage distributions

Recommended voltage distributions are given in the data sheets for each tube. As described earlier, see Fig.10, there are three main types:

- **type A**, iterative voltage distribution;
- **type B**, progressive voltage distribution;
- **type C**, intermediate progressive voltage distribution.

## Resistive dividers

Design of a resistive voltage divider depends on the supply voltage, the voltage distribution, and the anticipated mean anode current  $I_a$ . To ensure that voltage variations due to anode current variations are negligible, the nominal divider current  $I_d$  must be much larger than  $I_a$ ; a good rule is

$$\frac{I_d}{I_a} \geq 100$$

Consider a type C voltage distribution with  $V_{ht} = 2500$  V, (Fig.10), an interdynode voltage increment  $V_d$ , and a division ratio such that there are precisely 21.1 increments. Let the maximum anticipated mean anode current  $I_a$  be 10  $\mu$ A. The divider current  $I_d$  must then be at least 1 mA, which means a total divider resistance of 2.5 M $\Omega$  and an incremental resistor value of  $2.5 \times 10^6 / 21.1 \approx 120$  k $\Omega$ .

The resistors must be properly rated for power and voltage. The latter is important because some of them must withstand several hundred volts continuously. Tolerances should be not greater than 5%.

The  $I_d/I_a$  current ratio specified above represents a minimum for maintaining good linearity. Two other considerations limit the maximum value of the ratio.

- Heat due to dissipation in the divider ( $I_d^2 \cdot R$ ) can cause an increase in the dark current, especially if the divider and tube are housed close together or with the tube vertical, cathode uppermost.
- Low divider current affords a measure of protection against accidental overexposure of the cathode; as soon as

anode current rises proportionately, gain drops abruptly and prevents the anode current from becoming excessive (Fig.22).

## Transistorized dividers

To improve the stability of the last inter-stage voltages, transistors can be used instead of resistors (Fig.31). Using a standard resistive network limits the anode current to a few per cent of the divider current, so that the last inter-stage voltage drops are negligible.

Using transistors, however, allows the average anode current to be as high as half the divider current.

The divider current ( $I_d$ ) flows through the  $R_0$  to  $R_3$  chain, before splitting into two parts, according to the  $R_{N-4}$ ,  $R_{N-3}$  resistor values, (because the base-emitter voltage of transistor  $Q_1$  is close to zero,  $R_{N-4}$  and  $R_{N-3}$  are almost in parallel).

To simplify, suppose both resistors have the same value, then  $I_d/2$  flows through  $R_{N-4}$  and the chain of transistors, and  $I_d/2$  also flows through  $R_{N-3}$  to  $R_N$  ( $I_t \approx I_r$ ). The transistors are used as emitter-followers, which means their emitter voltages - and hence the last inter-stage voltages - follow the transistor base voltages. In other words, the inter-stage voltages are stable provided the base voltages are stable, which is true if the transistors have a high current gain ( $h_{fe} > 50$ ), so the base currents ( $I_b$ ) are negligible compared to  $I_r$ .

The transistors simply act as voltage sources irrespective of the collector current ( $I_c$ ), whose value ranges from  $I_d/2$ , when the anode current is zero, down to virtually zero when the anode current is close to  $I_d/2$ . The steady-state value of  $I_t$  gives the absolute maximum  $I_a$  the design can handle. A safety margin is recommended, to prevent  $I_a$  reaching the value of  $I_t$ .

Depending on the required average anode current, 2, 3 or more stages can be transistorized, since the last inter-stage voltages are the most affected by the anode current. Each design may also be optimized by experimenting with different  $R_{N-4}/R_{N-3}$  resistance ratios.

## Decoupling (Reservoir capacitors)

Provided the dynodes are adequately decoupled, instantaneous values of current in pulse operation may greatly exceed the mean value of the divider current. In observing the rule  $I_d/I_a \geq 100$ , the value taken for  $I_a$  should be the mean anode current based on the anticipated pulse amplitude and duty factor. Decoupling to restore the charge transferred by pulses passing through the tube may be either parallel, or series, Fig.32; the latter arrangement is often preferable as it enables capacitors with lower voltage ratings to be used.

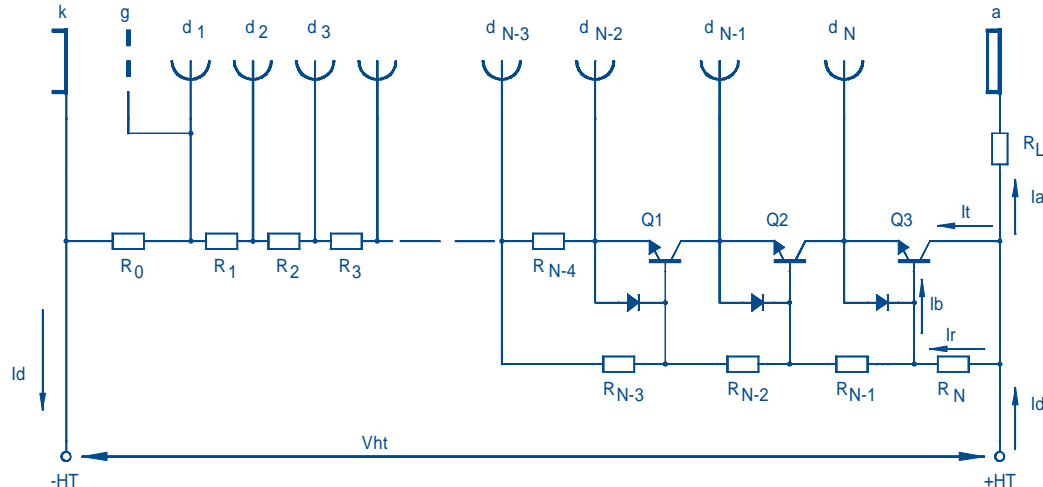


Fig.31 Using transistors to keep constant inter-electrode voltages on the last stages, even at high count rates.

These are smaller and less expensive than those for parallel decoupling.

The capacitance required is largest between the last dynode and anode, where the pulse amplitudes are largest, and decreases from stage to stage in proportion to the gain per stage. If  $q = I_a t$  is the maximum pulse charge to be delivered by the last dynode, and  $\Delta V$  the maximum voltage change that can be tolerated at that dynode, the capacitance required between the last dynode and anode is  $C = q / \Delta V$ .

### Example

The anode pulses expected in a given scintillation counting application have a maximum amplitude of 1 mA and a full-width at half maximum of 0.3  $\mu$ s, therefore,

$$q = 10^{-3} \text{ A} \times 0.3 \times 10^{-6} \text{ s} = 0.3 \times 10^{-9} \text{ coulomb.}$$

If the voltage difference between the last dynode and anode is 100 V and its maximum tolerable change is 1%, the required capacitance is then:

$$C_n = 1 \text{ V} \times 0.3 \times 10^{-9} \text{ C} = 0.3 \text{ nF.}$$

Assuming a stage-to-stage gain of 3, the capacitances needed in the preceding stages are

$$C_{n-1} = 0.1 \text{ nF}$$

$$C_{n-2} = 33 \text{ pF.}$$

Stages in which the capacitance is less than about 20 pF do not require reservoir capacitors; the stage-to-stage stray capacitance is usually sufficient.

If pulses occur in bursts there may be insufficient time between individual pulses to allow the reservoir capacitances to recharge fully. The effect of successive pulses is then cumulative and dynode voltages may change appreciably between the beginning and end of a burst, even though the long-term mean anode current is substantially less than  $I_d / 100$ . In that case, the voltage divider will have to be redesigned for a larger value of  $I_d$ .

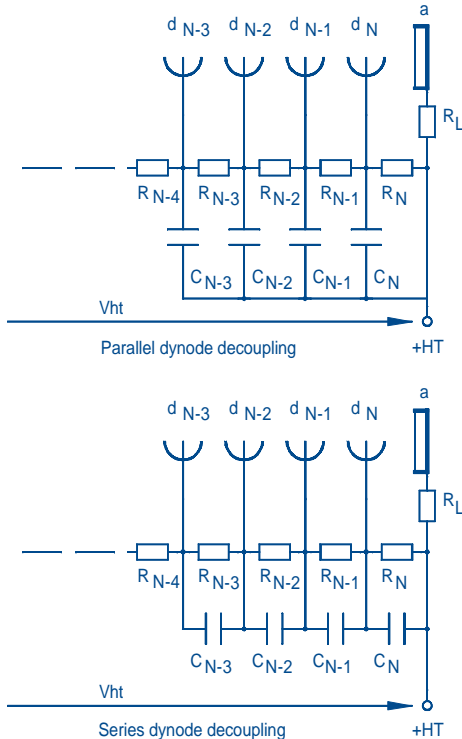


Fig.32 Parallel and series dynode decoupling.

### Anode resistor

Whether the tube is connected in positive or negative polarity, the anode potential must be fixed.

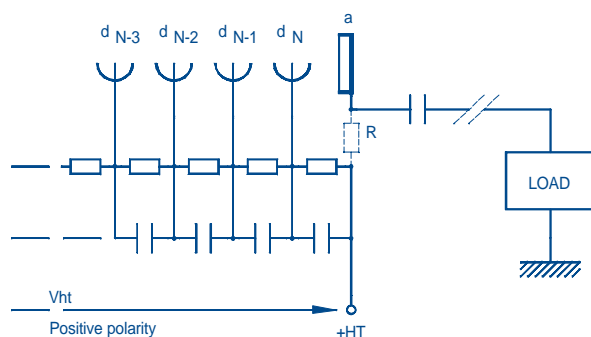
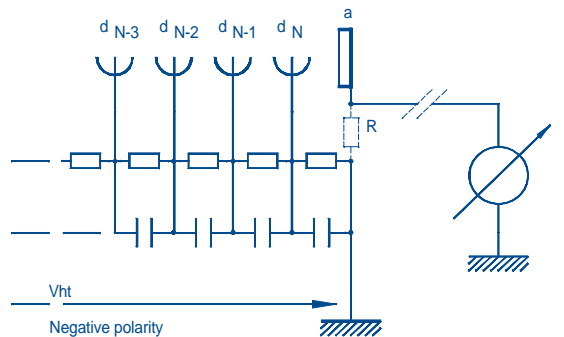


Fig.33 Fixing the anode potential with the tube connected in negative or positive polarity.

If the tube is connected in negative polarity and direct coupled to the measuring apparatus, the anode potential is clamped by the internal resistance of the apparatus. However, if the output is disconnected even briefly while the high voltage is still applied, the anode will acquire a negative charge which may damage the apparatus when connection is restored. Therefore it is advisable to fit a protection resistor (dotted in Fig.33) between the anode and earth.

As it is shunted across the high internal resistance of the photomultiplier, the protection resistance must also be high. The value chosen depends mainly on the load circuit and is typically  $\geq 10 \text{ k}\Omega$ .

If the tube is connected in positive polarity and capacitively coupled to the measuring circuitry, a resistor between the anode and the positive terminal of the high voltage supply is essential; this resistor can also constitute the anode load. Once again, the resistance must be reasonably high and depends mainly on the input impedance of the measuring circuitry.

### Gain adjustment

Gain characteristics differ from tube to tube. Sometimes, though, it is necessary to ensure that a number of tubes working together operate at equal gain. There are two ways to do this (Fig. 34).

### Supply voltage adjustment

Gain can be adjusted by adjusting the high voltage supplied to each tube. If the tubes do not have separately adjustable supplies but are fed from a common supply, their voltages can still be adjusted by ballast resistors connected in series with their respective voltage dividers. Even though the current from the supply is practically constant, the ballast resistors should be decoupled.

## Dynode voltage adjustment

This is often used when it is not practical to adjust the high voltage supply to each tube. Gain can be altered by altering the voltage of any dynode, but an intermediate one is always chosen to avoid interfering with the collection efficiency of the electron-optical input system or the output stage. Of the two adjustment circuits (shown in Fig.34), the (b) version is preferable if the divider current is high; it makes it possible to use a high-value potentiometer (about  $1\text{ M}\Omega$ ) with a low power rating ( $\leq 0.75\text{ W}$ ). In both the (a) and (b) versions, resistors should be connected on both sides of the potentiometer to limit its working voltage; in practice, the range of control variation required is usually far less than the maximum possible. As all terminals of the potentiometer are at a fairly high voltage, the potentiometer must be well insulated.

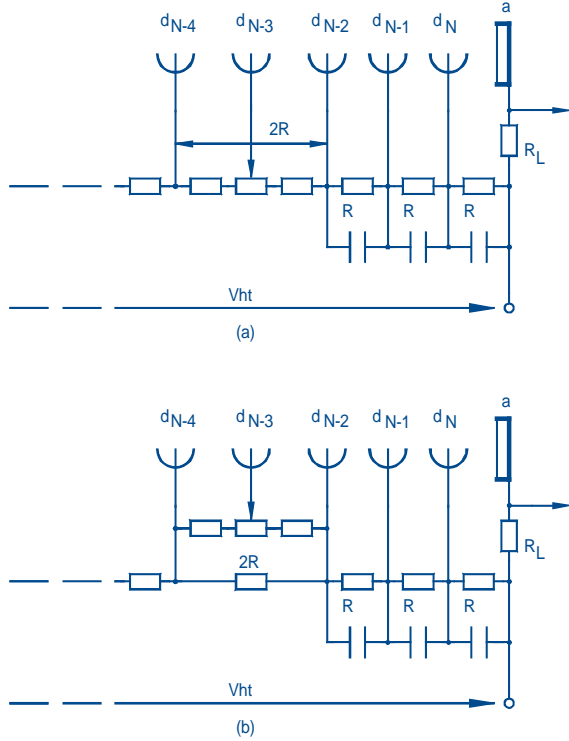


**Fig.34** Alternative circuits for adjusting gain by adjusting the voltage of one dynode.

Dynode voltage adjustment is more effective with focusing than with venetian-blind or foil dynodes. A disadvantage of it is that it can impair stability and increase susceptibility to magnetic fields; on the other hand, time characteristics are relatively unaffected.

## Supply for multiple tubes

When many photomultipliers are used together, the high voltage can be supplied either separately to each or by a single supply common to all.

## Separate supplies

Separate supplies are preferable. They prevent any reaction between tubes and, if they are adjustable, facilitate individual gain adjustment. Compact, adjustable and non-adjustable, individual supply modules are marketed, as well as supplies with several, separately adjustable output channels. The latter, though, are usually bulky and expensive.

## Common supply

Common supply to a number of tubes is often used when the current required from each is low. Each then has its own voltage divider to minimize reaction between tubes and its own provision for gain adjustment, which may be a potentiometer either

- in series with the divider (Fig.35);

- or controlling the voltage of one of the dynodes (Fig.36).

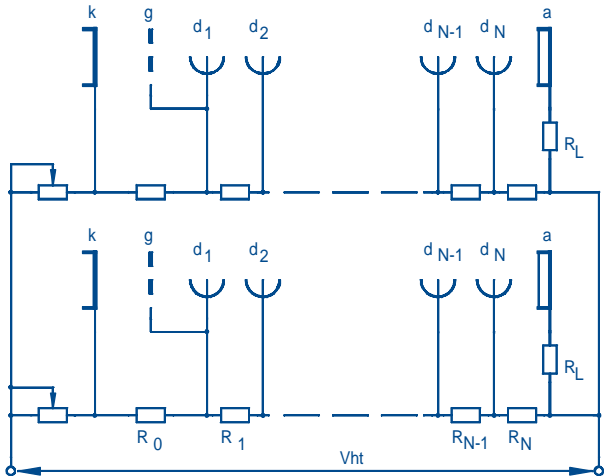


**Fig.35** High-voltage supply for photomultipliers in parallel.

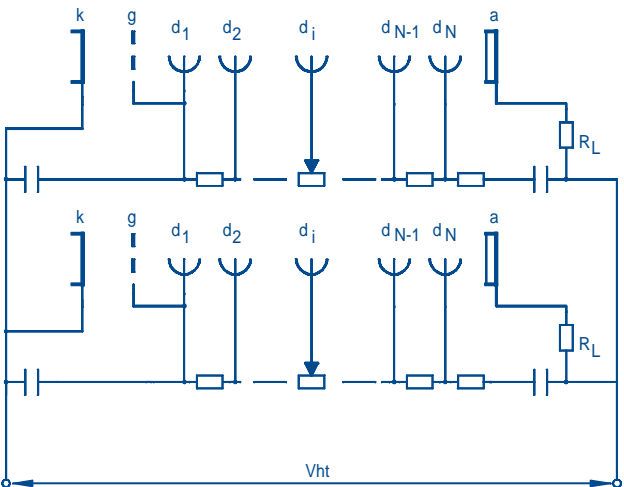


**Fig.36** High voltage supply for photomultipliers in parallel.

Placing a potentiometer in series with the resistor chain is a good solution particularly for tubes operated with the cathode at ground potential. For tubes operated with the anode at ground potential, the cathodes of each tube are at different potentials, so the tubes must be insulated from each other to prevent electrolysis phenomena (from voltages across tube walls) which may shorten tube life.

If a potentiometer is connected between the  $(i+1)$ th and  $(i-1)$ th dynodes to move the potential of the  $i$ th dynode away from its normal value, check that collection efficiency in the input stage is not degraded (which can happen when  $d_s$  is used) and that the linearity, and hence the dynamic range, remains at an acceptable level when the last dynodes are involved.

## Magnetic fields

Magnetic fields even as weak as the earth's affect photomultiplier performances. This can be demonstrated by rotating a horizontally mounted tube about its main axis. The resulting variation of anode sensitivity is due to the varying effect of the earth's field on the electron trajectories, and the corresponding variation of collection efficiency in all stages. Highly focused tubes, in which the electron impact areas on the dynodes are small, are the most sensitive to magnetic

effects; a transverse flux density of a few tenths of a millitesla can reduce gain by 50%. In a tube with venetian-blind dynodes, the field required to produce the same effect would be up to three times as large.

Magnetic influence is greatest in the electron-optical input system, where electron trajectories are longest. Increasing the voltage across the input system increases the energy of the electrons and decreases the sensitivity to magnetic fields.

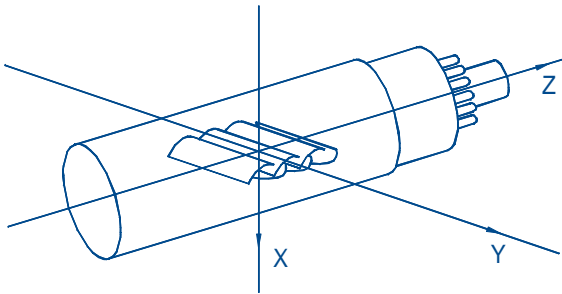


**Fig.37** Axes used in measuring magnetic sensitivity.

Tubes with linear-focusing dynodes are most sensitive to magnetic influence when the field is parallel to the dynodes (axis Y in Fig.37). Tubes with venetian-blind dynodes are least sensitive when the field is parallel to the axis of the tube.

Magnetic sensitivity is measured relative to three perpendicular axes (Figs 37 and 39).

Data sheets give either the measured sensitivity curves or the values of magnetic flux density parallel to each axis at which gain is halved. The data are for optimum operating conditions. Magnetic sensitivity is greater when electrode potentials are not optimum, as is the case when gain is deliberately decreased by defocusing a dynode or the accelerating electrode.

Strong fields may permanently magnetize some parts of a photomultiplier, lastingly affecting its performance. If that happens, the tube can be demagnetized with a coil producing a flux density of about 10 mT, at 50 Hz.

## Magnetic shielding

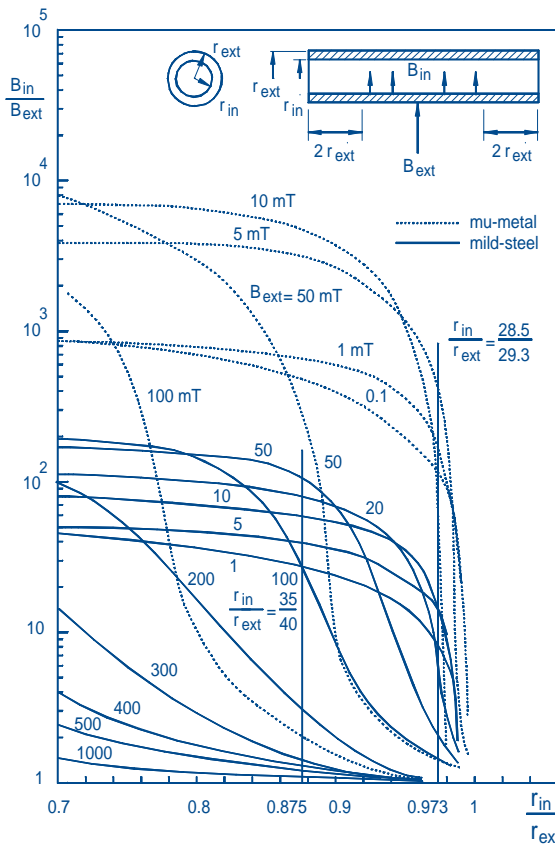


**Fig.38** Comparative effectiveness of mu-metal and soft iron magnetic shields.

Since fields as weak as the earth's can affect sensitivity, a mu-metal shield is always desirable. At flux densities of more than a few milliteslas, however, such a shield saturates and becomes ineffective. It must then be surrounded by a supplementary shield, usually of soft iron.

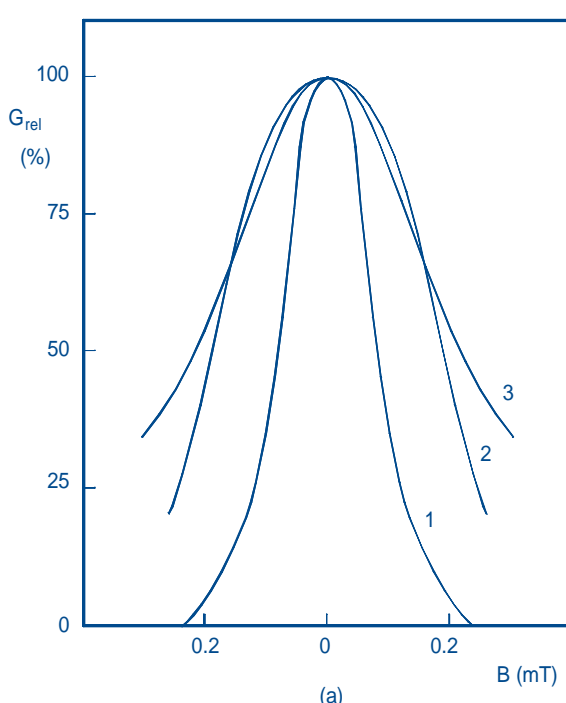
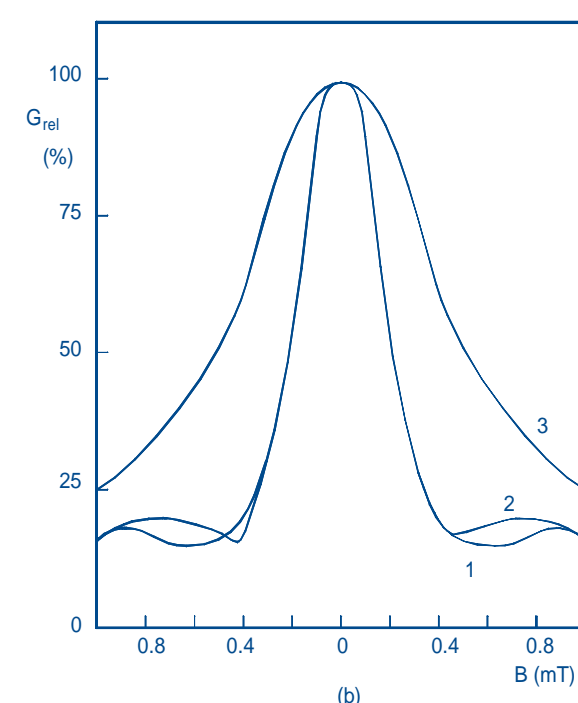


**Fig.39** Relative gain variation as a function of magnetic field for a tube with:  
(a) linear-focusing dynodes, and (b) with venetian-blind dynodes.

**Curve 1:** field aligned with y-axis (Fig.37).

**Curve 2:** field aligned with x-axis.

**Curve 3:** field aligned with z-axis.



Shielding effectiveness, based on material and dimensions, can be determined from Fig.38. For example, a mild-steel shield 70 mm in diameter and 5 mm thick ( $r_{in}/r_{ext} = 0.875$ ) in a flux density of 100 mT gives an attenuation of about 30. An inner mu-metal shield 57 mm in diameter and 0.8 mm thick ( $r_{in}/r_{ext} = 0.973$ ) gives an additional attenuation of about 300, leaving a residual flux density that is well below the 0.05 mT to 0.1 mT sensitivity threshold of most tubes.

Magnetic shields should extend about one diameter beyond the cathode plane, especially if the flux density is high. If the tube is operated in negative polarity, the shielding must be completely insulated from the glass or connected to the cathode potential via a protective resistor to prevent potential gradients across the glass wall causing electrolysis phenomena and permanent damage to the PMT photocathode.

## Environmental considerations

Environmental factors - chiefly temperature, magnetic fields, background radiation, and atmosphere - can affect the operation of a photomultiplier in varying degrees, temporarily or permanently. To a large extent the effects can be guarded against or compensated.

### Temperature

By the nature of their photoemissive and secondary emissive materials, photomultipliers are also sensitive to temperature variations. These affect three of the main characteristics:

- **spectral response** (the shape of the curve);
- **dark current** (the thermionic component);
- **anode sensitivity and gain** (secondary emission coefficients).

Changes in characteristics due to temperature variations within the permissible limits are usually reversible, though there may be some hysteresis that disappears only gradually.

Effects of temperature on the photoemission and secondary-emission surfaces are complex. They depend not only on the composition of the surfaces but also, to some extent, on the type of tube; and even between tubes of the same type there are appreciable differences. However, tendencies and average values can be identified. In storage as well as in use, photomultipliers must be kept within the temperature limits specified in their data sheets, usually -30°C to 80°C. Beyond those limits effects such as sublimation of the cathode or stresses in the glass may occur.

Specific tubes for high temperature are available (XP85051 and XP83092 families).

**Always consult PHOTONIS before considering operation of a photomultiplier outside its published temperature limits.**

### Effect on spectral sensitivity

The spectral sensitivity characteristic does not vary much with temperature. The greatest relative variation is usually observed close to the photoemission threshold. For a given application, therefore, it is advisable to choose a tube with a type of cathode that makes it possible to operate far from the threshold.

**Bialkali SbKCs cathode.** The temperature coefficient is very low in the wavelength range 400 nm to 500 nm where sensitivity is maximum, and may go to zero there or change sign. For temperature intervals -20°C to 20°C, and 20°C to 60°C, it is nowhere greater than 0.15% in the range 400 nm to 500 nm. Furthermore, its variation with temperature is very small at short wavelengths.

**Multialkali cathodes.** These are characterized by a negative temperature coefficient throughout most of the useful spectrum. Note that the ERMA type, whose response extends farther into the red, has a larger temperature coefficient than the standard multialkali type.

### Effect on cathode resistivity

The resistivity of photocathodes varies inversely with temperature. This can limit the minimum operating temperature, especially of bialkali SbKCs cathodes which, at room temperature, have a resistivity a hundred to a thousand times greater than that of multialkali cathodes (Fig.40). The practical minimum for bialkali cathodes is -20°C (if the cathode current is more than 0.1 nA).

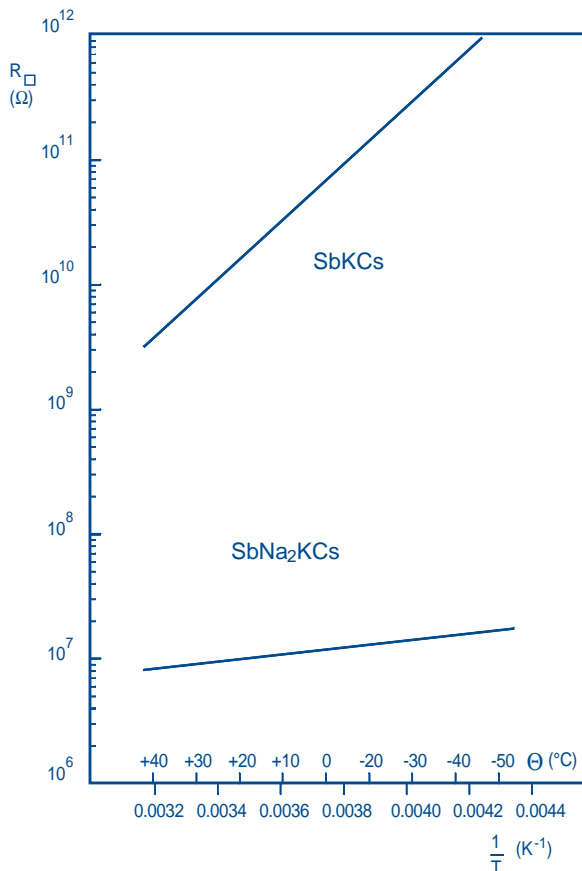


Fig.40 Surface resistivities of two photoemissive materials as functions of temperature.

### Thermionic emission characteristics of common photocathodes

type of cathode	thermionic emission at 20°C (A/cm <sup>2</sup> )	temperature rise for which thermionic current doubles (K)	minimum useful cooling temp. (°C)
AgOCs	$10^{-13} - 10^{-11}$	5 - 7	-100
SbKCs	$10^{-19} - 10^{-17}$	4 - 5	-20
SbNa <sub>2</sub> KCs	$10^{-19} - 10^{-15}$	4	-40
SbNa <sub>2</sub> KCs (ERMA)	$10^{-17} - 10^{-15}$	4	-40

## **Effect on the dark current**

The thermionic component of the dark current obeys Richardson's law, therefore, both dark current and dark pulse rate increase strongly with temperature. The rate of increase depends mainly on the cathode material but may differ considerably from one tube to another of the same type. This is because some components of the dark current, such as thermionic emission, field emission and leakage current have different temperature coefficients and differ in relative importance from tube to tube. For the same reason, the dark current and dark pulse rate do not usually continue to decrease below a certain temperature, and in some cases may even increase, particularly in tubes with multialkali cathodes.

## **Effect on gain and anode sensitivity**

Dynode secondary emission also varies with temperature (though less so than cathode thermionic emission) and correspondingly affects gain.

The temperature coefficient of gain is usually negative and depends not only upon the composition of the dynode surfaces, but also upon that of the cathode and, to some extent, the structure of the multiplier. For CuBe dynodes the coefficient is about -0.1% per degree with bialkali and trialkali cathodes. It is smaller in tubes with venetian-blind and foil dynodes than in those with focusing dynodes.

Variations in anode sensitivity reflect variations in both cathode sensitivity and multiplier gain. At certain temperatures and wavelengths these may be equal and opposite, cancelling each other.

## **Atmosphere**

### **Humidity**

Because of the high voltages used, operation in a damp atmosphere can lead to insulation problems. Condensation gives rise to leakage currents which increase the dark current. Local insulation breakdowns may also occur. Take particular care to avoid condensation on the glass, at the pins, and especially inside the plastic base. If moisture does get into the base, it will be necessary to drill a hole in the base key to enable it to escape.

### **Ambient pressure**

Photomultipliers can operate satisfactorily at low ambient pressure, but precautions against flashover at the pins are necessary at pressures below 10 kPa (175 torr). *For operation or storage at high ambient pressure, consult PHOTONIS; permissible pressures differ from type to type and are not usually given in the data sheets.*

### **Helium partial pressure**

Glass is permeable to helium, the rate of penetration being proportional to the helium partial pressure. Of the glasses used in photomultipliers, lime glass (soft glass) is the least permeable; borosilicate glass and fused silica (hard glasses) are, respectively, about 100 and 1000 times more permeable. Helium intrusion increases the afterpulse factor and shortens the life: a tube with a fused silica window in a helium partial pressure of 100 kPa has a useful life of only a few days; this is a hazard to be guarded against in helium-cooled high-energy physics experiments. The partial pressure of atmospheric helium is normally about 0.7 Pa, which is low enough to allow an average useful life of some ten years. Finally, note that helium penetration increases with temperature.

## **Mechanical stress**

Like all electron tubes, photomultipliers should be protected against undue mechanical and temperature stress. Vibration or shock transmitted to the dynodes can modulate the gain (microphony).

## **Radiation**

Permanent loss of gain and sensitivity is a serious risk only in very high radiation environments, such as parts of extraterrestrial space where electron flux can reach  $10^{10}$  electrons per square centimetre per second, and in high-energy physics experiments. Under those conditions the emissive properties of the dynodes change and the input window darkens, affecting the transmission at shorter wavelengths. Lime glass windows are more sensitive than others to prolonged radiation. The thin photoemissive layer is relatively unaffected, probably because its absorption coefficient for ionizing radiation is low.

In case photomultiplier tubes are used in a high radiation environment, this may lead to a degradation of the transmission coefficient of the window. Some studies have been made (K.W. Bell & al. NIM section A469 (2001) 29-46 *The development of vacuum phototriode for the CMS electromagnetic calorimeter*) and shown that UV-transparent borosilicate is a suitable glass for this purpose.

Permanent alteration of gain and sensitivity becomes noticeable only after exposure doses of about  $10^4$  rad.

## **Reference**

*Photomultiplier tubes: Principle & Applications,*  
Photonis, 2002, PHOTONIS ordering code D-PMT-AB2002.  
(Available from PHOTONIS and representatives.)